Reversible Notch1 acetylation tunes proliferative signalling in cardiomyocytes

Chiara Collesi[1,2,3]*, Giulia Felician[1†¶], Ilaria Secco[1¶], Maria Ines Gutierrez[1], Elisa Martelletti[1‡], Hashim Ali[1], Lorena Zentilin[1], Michael P. Myers[4], and Mauro Giacca[1,2,3]*

[1]Molecular Medicine Laboratory, International Centre for Genetic Engineering and Biotechnology (ICGEB), Padriciano 99, 34149 Trieste, Italy; [2]Department of Medical, Surgical and Health Sciences, University of Trieste, Strada di Fiume 447, 34100 Trieste, Italy; [3]Center for Translational Cardiology, Azienda Sanitaria Universitaria Integrata, Via Valdoni 7, 34100 Trieste, Italy; and [4]Protein Networks Laboratories, International Centre for Genetic Engineering and Biotechnology (ICGEB), Padriciano 99, 34149 Trieste, Italy

Accepted 23 November 2017

Aims The Notch signalling pathway regulates the balance between proliferation and differentiation in several tissues, including the heart. Our previous work has demonstrated that the proliferative potential of neonatal cardiomyocytes relies on Notch1 activity. A deep investigation on the biochemical regulation of the Notch signalling in cardiomyocytes is the focus of the current research.

Methods and results We show that the Notch1 intracellular domain is acetylated in proliferating neonatal rat cardiomyocytes and that acetylation tightly controls the amplitude and duration of Notch signalling. We found that acetylation extends the half-life of the protein, and enhanced its transcriptional activity, therefore counteracting apoptosis and sustaining cardiomyocyte proliferation. Sirt1 acted as a negative modulator of Notch1 signalling; its overexpression in cardiomyocytes reverted Notch acetylation and dampened its stability. A constitutively acetylated fusion protein between Notch1 and the acetyltransferase domain of p300 promoted cardiomyocyte proliferation, which was remarkably sustained over time. Viral vector-mediated expression of this protein enhanced heart regeneration after apical resection in neonatal mice.

Conclusion These results identify the reversible acetylation of Notch1 as a novel mechanism to modulate its signalling in the heart and tune the proliferative potential of cardiomyocytes.

Keywords Acetylation • Adeno-associated virus (AAV) • Cardiac apical resection • Cardiomyocytes • Notch1 • Sirt1

1. Introduction

In the mammalian heart, cardiomyocytes actively proliferate during embryonic development, but stop dividing and make a transition from hyperplastic to hypertrophic growth shortly after birth.[1–3] Despite recent evidence that new myocyte formation takes place in the adult heart,[4–6] cell cycle activity is very low in adult cardiomyocytes and myocardial repair after damage occurs through scarring and fibrosis,. which frequently leads to heart failure. Despite remarkable progress in the use of devices assisting the failing myocardium,[7] the prognosis of this condition remains very poor, with mortality estimated at 40% of patients at 4 years from diagnosis.[8] Thus, the identification of molecular strategies capable of inducing cardiac tissue regeneration by sustaining cardiomyocyte generation and expansion appears to be of paramount importance

One of the essential determinants of cardiomyocyte proliferation during development is the activity of the Notch pathway. In mammals, Notch signalling occurs after the interaction of one of the four Notch receptors (Notch1–4) with membrane-bound ligands of the Jagged (Jagged1 and 2) and Delta-like (Delta-like1, 3, and 4) family. Interaction between Notch and its ligands induces proteolytic processing of the receptor, which results in the release of the protein intracellular domain (Notch-ICD), followed by its nuclear translocation and interaction with

* Corresponding authors. Tel: +39 040 375 7375; fax: +39 040 375 7380, E-mail: collesi@icgeb.org (C.C.); Tel: +39 040 3757324; fax: +39 040 3757380, E-mail: giacca@icgeb.org (M.G.)

† Present address. Technische Universität München, Institute of Pharmacology and Toxicology, Munich, Germany

‡ Present address. King's College London, Wolfson Centre for Age-Related Diseases, London, UK

¶ These authors contributed equally to this work.

the transcription factor CSL and various co-activators that regulate chromatin organization, such as PCAF, GCN5, p300, and MAML, which are recruited to trigger the transcription of genes of the hairy and enhancer of split (HES), family (reviewed in Refs.[9–11]).

Notch signalling is active in the embryonic heart of multiple species, where it influences cell fate and morphogenesis, including commitment between the mesodermal and neuroectodermal lineages, establishment of the atrioventricular canal myocardial boundary and epithelial-to-mesenchymal transition during heart valve development.[12–14] Most notably, Notch essentially regulates cardiomyocyte proliferation during development and in the early postnatal life. In particular, we and others have shown that the Notch pathway sustains the proliferation of committed precursors and immature cardiomyocytes,[15–18] and is essential for the maintenance of the heart structural and functional integrity after myocardial infarction[19,20] during the response to increased workload[16] or during heart failure.[21] In other species that efficiently regenerate the heart after damage, in contrast to mammals, Notch is also essential for postnatal cardiomyocyte proliferation,[22,23] while recent evidences from our laboratory have demonstrated that it is largely ineffective in driving cardiac regeneration in adults, because of permanent epigenetic modification at main Notch-responsive promoters.[24]

As only modest differences in the Notch pathway activity suffice to determine dramatic differences in cellular behaviour, this pathway appears to be tightly regulated by a variety of molecular mechanisms, including post-translational modification.[25] In particular, work performed in endothelial cells has revealed that acetylation of the Notch-ICD finely tunes Notch signalling, by increasing protein stability in this cell type.[26] The positive role of acetylation is opposed by the class III, NAD^+-dependent histone deacetylase Sirt1, an enzyme known to be involved in diverse biological processes, ranging from metabolism to aging and cancer.[27–29]

We report here that the Notch1-ICD is acetylated in neonatal rat cardiomyocytes, and that acetylation tightly controls the amplitude and duration of Notch signalling by counteracting proteasomal degradation of the protein. We found that Sirt1 acts as a negative modulator of Notch1 signalling; its overexpression in cardiomyocytes reverted Notch-ICD acetylation and reduced its stability. We generated Adeno-Associated Virus serotype 6 (AAV6) vectors expressing the Notch1 intracellular domain (N1ICD), its isoform devoid of the PEST domain [N1ICD(ΔC)] and a fusion protein between the N1ICD and the catalytic domain of p300 [N1ICD(ΔC)-HAT]. Expression of this fusion protein expanded the proliferation window of transduced neonatal cardiomyocytes, which were able to undergo cell division up to 2 weeks after plating. AAV9-mediated delivery of this chimeric factor in neonatal mouse hearts after apical resection boosted cardiomyocyte proliferation and enhanced myocardial regeneration. These results identify the reversible acetylation of Notch1 as a novel mechanism to tune the proliferative potential of postnatal cardiomyocytes both *in vitro* and *in vivo*.

2. Methods

2.1 Animals

Wistar rats and CD1 mice were purchased from Charles River Laboratories Italia Srl and maintained under controlled environmental conditions. Animals were housed and handled according to institutional guidelines in compliance with national and international laws and policies. Experimental procedures were approved by the ICGEB Animal Welfare Board and Ethical Committee, with full respect to the EU Directive 2010/63/EU for animal experimentation.

2.2 Surgical procedures

Heart apical resection was performed as described in Ref.[30] Briefly, neonatal mice were anaesthetized for 4 min on ice. Thoracotomy was performed, followed by resection of ~15–20% of the ventricle, involving exposure of the left ventricular chamber. For sham operations, we performed thoracotomy without apical resection. Sham and resected animals were sutured and allowed to recover under a heat lamp for several minutes until the end of anaesthesia. Approximately 70% of animals undergoing apical resection survived surgery. Resections larger than 20% typically resulted in lethality. The day after surgery, survived animals were injected intraperitoneally using a tuberculin syringe (30 G; Roche) with AAV9-Control, AAV9-N1ICD, AAV9-N1ICD(ΔC), AAV9-N1ICD(ΔC)-HAT at a dose of 2.5×10^{10} vg per g of body weight. Neonates sacrificed 7 days after surgery were injected with BrdU (25 mg/kg body weight) 48 h prior to sacrifice; animals sacrificed 21 days after apical resection received BrdU injection both at Day 15 and 19 after surgery.

2.3 Heart collection and immunohistological analysis

At the end of the studies, animals were anaesthetized with 5% isoflurane and euthanized by cervical dislocation. Hearts were excised, briefly washed in phosphate buffered saline (PBS), snap frozen or fixed in 10% formalin and embedded in paraffin for immunofluorescence or histological analysis. For each heart, paraffin sections (4 μm) were collected from 5 to 7 regions throughout the heart, de-paraffinized and rehydrated. Antigen retrieval was performed in 0.1 M sodium citrate buffer at pH 6.0. Samples were permeabilized 30 min in 0.5% Triton X100 and blocked for 1 h in 2% bovine serum albumin (BSA) in PBS. BrdU staining was performed according to the manufacturer's instructions (BD Biosciences). Sections were stained overnight at 4 °C with the following primary antibodies diluted in blocking solution (2% BSA): mouse anti α-sarcomeric actinin (EA-53) 1:250 (AbCam), rat monoclonal anti-BrdU (BU1/75) 1:100 from AbCam, rabbit polyclonal anti-histone H3 phosphorylated at serine 10 (06-570) 1:100 from Millipore. Goat anti-mouse conjugated to Alexa Fluor 488; goat anti-rabbit conjugated to Alexa Fluor 594; goat anti-rat conjugated to Alexa Fluor 594 were used as secondary antibodies. Nuclei were stained with DAPI (H-1, 200, Vector laboratories). For each section, we averaged the number of BrdU+/α-actinin+ and pH3+/α-actinin+ cells across 10 fields taken around the left ventricle and the septum, which were both damaged during the resection procedure. Blinded quantification was performed on images taken at 40× magnification. Masson's trichrome staining (Thermo Scientific, No. 87019) was performed following the manufacturer's protocol. A total of six animals per group were analysed.

2.4 Culture of neonatal rat cardiomyocytes

Ventricular cardiomyocytes were isolated as described previously in Ref.[15] In brief, ventricles from neonatal rats (post-natal Day 1), sacrificed by rapid decapitation, were separated from the atria, cut into pieces and then dissociated in CBFHH (calcium and bicarbonate-free Hanks with Hepes) buffer containing 2 mg/mL of trypsin (BD Difco, Franklin Lakes, New Jersey, USA) and 20 μg/mL of DNase II (Sigma, St. Louis, USA), under constant stirring. Digestion was performed at room temperature in eight to ten 10-min steps, collecting the supernatant to fetal bovine serum (FBS, Life Technologies, Carlsbad, CA, USA) after each step. The collected supernatant was centrifuged to separate the cells, which were then resuspended in Dulbecco's modified Eagle medium 4.5 g/L glucose (DMEM, Life Technologies) supplemented with 5% FBS, 20 μg/

mL vitamin B12 (Sigma), 100 U/mL of penicillin and 100 μg/mL of streptomycin (Sigma). The collected cells were filtered through a cell strainer (40 μm, BD Falcon) and then seeded onto uncoated 100-mm plastic dishes for 2 h at 37 °C in 5% CO_2 and humidified atmosphere. The supernatant, composed mostly of cardiomyocytes, was then collected and pelleted. Cells were counted and plated at the appropriate density; cultures of neonatal rat ventricular CMs prepared using this procedure yielded consistently a purity of >90%.

In the experiments requiring AAV-mediated gene transfer, neonatal rat cardiomyocytes were infected at an MOI of 5×10^3 viral genomes (vg)/cell immediately after isolation. Twelve hours later, the culture medium was changed and cells were subjected to the different treatments and subsequent analyses.

2.5 Soluble-Jagged1 stimulation of neonatal rat cardiomocytes

Conditioned media from subconfluent pCDNA3.1-sJ1 and pMexNeo NIH-3T3 stable transfectants were prepared as described in Ref.[15] For the different assays, rat cardiomyocytes were fed in serum-free medium supplemented with 20× concentrated sJ1 or pMexNeo supernatants, then subjected to analysis at the indicated time points.

2.6 Cell culture and drugs treatments

HEK293T cells were purchased from ATCC and cultured in DMEM containing 10% FBS (Gibco, Billings, Montana, USA). Both rat neonatal cardiomyocytes and HEK293T transfected cells were treated with 0.5 μM trichostatinA (TSA; Calbiochem), 20 mM nicotinamide (NAM; Sigma), 1 μM (S)-35 (Santa Cruz), 30 μM resveratrol (resv; Sigma). Control groups were treated with respective vehicles.

2.7 Constructs, chemicals, and antibodies

The pCDNA3-N1ICD-V5 and the pCDNA3-N1ICD14KR-V5 plasmids were provided by M. Potente (Institute for Cardiovascular Regeneration, Centre of Molecular Medicine, Goethe University, D-60590 Frankfurt, Germany); pCS2-ICV-6MT plasmid, kindly provided by R. Kopan (Molecular Biology and Pharmacology, Washington University, St. Louis, MO, USA), was subcloned both in pCDNA3 and pAAV (Stratagene). SIRT1 cDNA was kindly provided by F. Ishikawa (Laboratory of Molecular and Cellular Assembly, Department of Biological Information, Graduate School of Bioscience and Biotechnology, Tokyo Institute of Technology, 4259 Nagatsuta, Midori-ku, Yokohama 226-8501, Japan; Laboratory of Cell Cycle Regulation, Department of Gene Mechanisms, Graduate School of Biostudies, Kyoto University, Kitashirakawa Oiwake-cho, Sakyo-ku, Kyoto 606-8502, Japan) and subcloned in pAAV (Stratagene, La Jolla, CA, USA); pASK-IBA37-HATwt and pASK-IBA37-HATmut were kindly provided by A. Cereseto (CIBIO, Università di Trento, Italy); wild type (4xwtCBF1Luc) and mutant (4xmtCBF1luc) reporters were provided by S.D. Hayward (John Hopkins University School of Medicine, Baltimore, MD, USA); the pHes1-Luciferase reporter construct was provided by R. Kageyama (Institute for Virus Research, Kyoto University, Kyoto, Japan); the insertless pMEXneo and sJ1 constructs, together with stable NIH-3T3 transfectants, were provided by I. Prudovsky (Center for Molecular Medicine, Maine Medical Center Research Institute, Scarborough, ME, USA). 5-Ethynyl-2′-deoxyuridine (EdU) was obtained from Boehringer-Mannheim/Roche, Basel, Switzerland. Hoechst 33258, RNase A, and all other chemicals were purchased from Sigma-Aldrich.

Three polyclonal antisera were obtained, specific for the acetylated N1ICD, by immunizing rabbits with peptides (named Ac-Peptide1, Ac-Peptide2, Ac-Peptide3) having the amino acid sequence 1761-$_{AC}$EGF**K$_{AC}$**VSEAS**K$_{AC}$K$_{AC}$K$_{AC}$**RREPLG-C-1778, 2144-$_{AC}$QG**K$_{AC}$K$_{AC}$**AR**K$_{AC}$**PST**K$_{AC}$**GLASGS**K$_{AC}$**EA**K$_{AC}$**DLK-C-2167, 2065-$_{AC}$ETA**K$_{AC}$**VLLDHFA-C-2075 respectively, followed by IgG purification with the Immunopure IgG Purification kit (Pierce, Waltham, Massachusetts, USA). The purified IgG fraction of antibodies specific to total Notch1 was purified by chromatography on SulfoLink Coupling Gel (SulfoLink kit; Pierce) coupled to the unmodified peptides. The flow-through fraction was further purified by affinity chromatography by coupling the acetylated peptides to another SulfoLink Coupling Gel column; the ac-Notch1-specific antibodies were eluted in IgG elution buffer and neutralized to pH 8.0; 1% BSA was added as a stabilizer. Serial dilutions of both acetylated (Ac-Pep1, Ac-Pep2, and Ac-Pep3) and not acetylated Notch1 peptides (Pep1, Pep2, and Pep3) were blotted on a Protran BA79 membrane, 0.1-mm pore size. The membrane was air-dried, blocked it in 5% BSA in TBS-Tween 0.1% and incubated overnight with the affinity-purified ac-Notch1-specific antibodies. The same membrane was stripped and then incubated with the total Notch1 specific IgGs.

2.8 Immunoprecipitation and western blot analysis

To detect acetylated N1ICD, 1×10^6 neonatal rat cardiomyocytes were plated in 60 mm primary cells culture dishes (BD) and grown in the presence of 0.5 μM TSA, 20 mM NAM, 1 μM S(-35), or 30 μM resveratrol and the respective vehicles for 8 h prior to protein analysis. Cells were lysed in IPLS buffer (Immuno-Precipitation-Lysis-Buffer-50 mM Tris–HCL pH 7.5, 120 mM NaCl, 0.5 mM EDTA, and 0.5% Nonidet P-40) supplemented with 10 μM TSA, 20 mM NAM, 10 mM sodium butyrate, 90 μg/mL PMSF (Phenylmethanesulfonyl fluoride), 1 mM $NaVO_4$ (all from Sigma) and proteases inhibitors (Roche). After sonication and preclearing, proteins concentration was determined by Bradford Assay (Biorad). N1ICD was immunoprecipitated from total cell lysates with 1 μg/mL of activated Notch1 antibody (Val 1744, Cell Signalling) or direct-conjugated immuno-affinity agarose beads against HA (Sigma), Myc (Sigma), or V5 (Invitrogen) for 2 h at 4 °C with gentle rotation, followed by incubation with protein A/G agarose beads (Santa Cruz) for additional 2 h. Immunoprecipitates were resolved on 6% SDS–PAGE minigels and transferred to nitrocellulose membranes (GE Healthcare). Immunoblots were blocked in 5% BSA (Roche) in TBST (50 mM Tris–HCl, pH 7.4, 200 mM NaCl, and 0.1% Tween 20). Membranes were incubated with primary antibodies overnight and washed in Tris-buffered saline, 0.1% Tween 20. Secondary antibodies were diluted in blocking buffer and incubated with the membranes for 45 min at room temperature. Proteins were detected with the ECL detection kit (GE Health Care Bio-Sciences). Western blotting was performed with polyclonal anti-acetylated lysine antibodies (AcK, 1:1000, Cell Signalling), or the Acetylated-Notch1 antibody #2B (1:1000), or with antibodies against Flag (1:1000, Sigma), V5 (1:5000, Sigma), HA (1:2000, Roche), anti-Myc epitope (1:1000, 9E10, Santa Cruz) Notch1 (1:1000, C-20, Santa Cruz), activated Notch1 (Val1744-1:1000, Cell Signalling), human Sirt1 (1:1000, MILLIPORE), tubulin (1:5000, Sigma), nuclear matrix protein p84 (1:1000, AbCam). Membrane stripping was performed in stripping buffer (100 mM 2-mercaptoethanol, 2% SDS, 62.5 mM Tris–HCl pH 6.7) at 56 °C for 15 min, followed by extensive washing in TBST.

2.9 Subcellular fractionation

Neonatal ventricular rat cardiomyocytes were washed once with PBS and scraped from the cell plate into hypotonic buffer (10 mM Hepes-KOH, 10 mM NaCl, 1 mM KH_2PO_4, 5 mM $NaHCO_3$, 1 mM $CaCal_2$, and 0.5 mM $MgCl_2$). After a 5-min incubation on ice, cells were spun at 1000 *g* for 5 min. The supernatants from this low-speed centrifugation were spun at 100 000 *g* for 90 min at 4° C to generate the cytosolic fraction. The pellet of the low-speed centrifugation was washed twice in PBS and resuspended with nuclear isolation buffer (10 mM Tris, pH 7.5, 300 mM sucrose, 0.1% Nonidet P-40). After 5 min of incubation on ice, 1% Triton X-100 was added, to generate the nuclear fraction. The buffers used in the subcellular fractionation were supplemented with 10 μM TSA, 20 mM NAM, 10 mM sodium butyrate, 90 μg/mL PMSF, 1 mM $NaVO_4$ (all from Sigma) and proteases inhibitors (Roche). Proteins of both cytosolic and nuclear fractions were subjected to further analyses as described above.

2.10 Analysis of protein stability

Notch1 protein stability was tested in neonatal cardiomyocytes treated with 0.5 μM TrichostatinA (TSA; Calbiochem), 20 mM nicotinamide (NAM; Sigma), 1 μM (S)-35 (Santa Cruz), 30 μM resveratrol (resv; Sigma) for 8 h. The medium was then supplemented with 10 μg/mL cycloheximide (CHX; Calbiochem) for 1, 2, 3, and 4 h prior to cell lysis in RIPA Buffer (Radioimmunoprecipitation assay buffer, 50 mM Tris–HCl, 150 mM NaCl, 5 mM EDTA, 5 mM EGTA, 0.5% NaDoc, 1% Triton X-100, and 0.1% SDS) supplemented with 10 μM TSA, 20 mM NAM, 10 mM sodium butyrate, 90 μg/mL PMSF, 1 mM $NaVO_4$ (all from Sigma), and proteases inhibitors (Roche). The proteasome inhibitor MG132 (Calbiochem) was supplemented at a concentration of 10 μM for 4 h. After sonication and pre-clearing, proteins concentration was determined by Bradford Assay (BIORAD). Equal amounts of protein were resolved on 6% SDS–PAGE minigels and transferred to nitrocellulose membranes (GE Healthcare). Western blotting was performed as described above, using a polyclonal Notch1 antibody (C-20-1:1000, Santa Cruz).

2.11 RNA isolation and quantitative real-time PCR

Total mRNA was purified from cultured neonatal cardiomyocytes transduced with either Control or AAV6-N1ICD, AAV6-N1ICD(ΔC), N1ICD(ΔC)-HAT, and AAV6-SIRT1 vectors (MOI = 5×10^3 vg/cell) or from total heart homogenates using miRNeasy Mini Kit (Qiagen), according to the manufacturer's instructions. Quantification of gene expression was performed by quantitative real-time PCR using the primers listed in Supplementary material online, *Table S2*. The housekeeping gene HPRT was used for normalization. The amplifications were performed using a BIORAD CFX96 machine using GoTaq qPCR Master Mix (Promega). The real-time qPCR program was performed with a melting curve dissociation protocol (from 60 °C to 95 °C), according to manufacturer's instruction. The final dilution of the primers in the reaction was 900 nm; for each primer set, optimal conditions were established and efficiency of the amplification was calculated.

2.12 Luciferase assay

To detect Notch1 activity under different experimental conditions, neonatal cardiomyocytes were seeded onto 96-well primary cells culture plates (1×10^5 cells per well) and co-transfected after either 2 or 6 days after isolation with 0.5 μg of either pHes1 or CBF1-Luc reporter plasmids and 0.01 μg pRL-Renilla (which was used as a control) by using Lipofectamine 2000 transfection reagent (Invitrogen). After incubation for 6 h, medium was removed and cells were fed in serum-free medium with either sJ1 or pMex-Neo concentrated supernatants, or treated with 0.5 μM TSA, 20 mM NAM, 1 μM S(-35), 30 μM resveratrol for 8 h prior to lysis. Firefly luciferase activity was corrected for the transfection efficiency by using the control Renilla luciferase activity in each sample. Firefly and Renilla luciferase activities were assayed with the Dual-luciferase assay kit (Promega, Madison, Wisconsin, USA).

2.13 Caspase 3/7 assay

For apoptosis analysis *in vitro*, at 2 or 6 days after cardiomyocyte isolation, cells were grown in DMSO-(Control) or DAPT containing medium (20 μM) and treated with 0.5 μM TSA, 20 mM NAM, 1 μM S(-35), or 30 μM resveratrol for 8 h prior to the analysis. Caspase 3/7 Glo assay (Promega) was performed, according to the manufacturer's instructions.

2.14 Cell proliferation assay

Cardiomyocyte proliferation was analysed 3, 7, and 12 days after their isolation. Cells were grown in culture medium supplemented with 5 μM 5-ethynyl-2′-deoxyuridine (EdU, Life Technologies) and in the presence of either 0.5 μM TSA, 20 mM NAM, 1 μM S(-35), or 30 μM resveratrol for 8 h. Cells were processed for immunofluorescence using the Click-IT EdU 555 Imaging kit to reveal EdU incorporation, according to the manufacturer's instructions. For the BrdU incorporation assays, 3, 7, and 12 days after isolation, cells were transduced with AAV6-MCS (Control), AAV6-N1ICD, AAV6-N1ICD(ΔC), N1ICD(ΔC)-HAT, or AAV6-SIRT1 (MOI = 5×10^3 vg/cell) and grown in culture medium supplemented with 10 μM Bromodeoxyuridine (BrdU, Boehringer-Mannheim/Roche) for 8 h prior fixation. BrdU staining was performed according to the manufacturer 's instructions (BD Biosciences).

2.15 Immunocytochemical staining

Cells were fixed with 4% paraformaldehyde for 10 min, permeabilized with 0.1% Triton X-100 in PBS for 10 min, followed by 1 h blocking in 2% BSA (Roche) in PBS. Cells were then stained over night at 4 °C with the following primary antibodies diluted in blocking solution: rabbit polyclonal anti-Acetylated Notch1 (#2B), 1:100; mouse anti α-sarcomeric actinin (EA-53), 1:250 (AbCam), rat monoclonal anti-BrdU 1:100 (BU1/75, AbCam), rabbit polyclonal anti-histone H3 phosphorylated at serine 10 1:100 (06-570, Millipore), rabbit polyclonal anti-Aurora B kinase 1:100 (ab2254, Abcam). Cells were washed with PBS and incubated for 1 h with the respective secondary antibodies goat anti-mouse conjugated to Alexa Fluor 488; goat anti-rabbit conjugated to Alexa Fluor 594; goat anti-rat conjugated to Alexa Fluor 594. All washes were in PBS 0.2% Tween 20. When indicated, cells were further processed using the Click-IT EdU 555 Imaging kit to reveal EdU incorporation, according to the manufacturer's instructions, and stained with Hoechst 33342 (Life Technologies).

2.16 Image acquisition and analysis

Image acquisition was performed using an ImageXpress Micro automated high-content screening fluorescence microscope at ×10 magnification; a total of 16 images were acquired per wavelength, well and replicate, corresponding to approximately 2500 cells analysed per condition and replicate. Image analysis was performed using the Multi-Wavelenght Cell Scoring application module implemented in MetaXpress software (Molecular Devices). In all quantifications, cardiomyocytes were distinguished from other cells present in the primary

cultures by their positivity for sarcomeric α-actinin. Visualization of acetylated Notch1ICD in cardiomyocytes was performed by manual inspection and counting of 15 images acquired per well, at a 40× magnification. Images were acquired at room temperature with a DMLB upright fluorescence microscope (Leica) equipped with a charge-coupled device camera (CoolSNAP CF; Roper Scientific) using MetaView 4.6 quantitative analysis software (MDS Analytical Technologies). For image acquisition, the following objectives were used: HCX PL Fluotar 100×/1.30 NA, HCX PL apocromatic 63×/1.32–0.6 NA, HCX PL Fluotar 40×/0.75 NA, HCX PL N-Plan 20×/0.40 NA, and HCX PL N-Plan 10×/0.25 NA (all from Leica). Within each experiment, instrument settings were kept constant.

2.17 Proteomic analysis

HEK293 (1×10^7) cells were transfected with 50 µg of N1ICD(ΔC)-HAT or N1ICD(ΔC)-D1395YHAT tagged fusion proteins and grown in the presence of 20 mM NAM or 0.5 µM TSA for 8 h prior to protein extraction. Tagged proteins were immunoprecipitated and processed for analysis by LC-MALDI mass spectrometry as described Ref.[31] The resulting spectra were analysed using the X! tandem search engine using the ENSEMBL mouse protein database (release GRCm37).

2.18 Production, purification, and characterization of recombinant AAV vectors

Recombinant AAV (rAAV) vectors were prepared by the AAV Vector Unit at the International Centre for Genetic Engineering and Biotechnology Trieste (http://www.icgeb.org/RESEARCH/TS/COREFACILITIES/AVU.htm), as described previously in Ref.[32] In brief, infectious AAV6 vector particles were generated in HEK293 cells by co-transfecting each vector plasmid [pAAV-N1ICD-Myc, pAAV-N1ICD(ΔC)-Myc, pAAV-N1ICD(ΔC)HAT-Ha, pAAV-SIRT1, and pAAV-MCS] together with the packaging plasmid [pAAV6-2[33]; and helper plasmid (pHELPER; Stratagene)], expressing AAV and adenovirus helper functions, respectively. Viral stocks were obtained by $CsCl_2$ gradient centrifugation; rAAV titers, determined by measuring the copy number of viral genomes in pooled, dialyzed gradient fractions, as described previously,[34] were in the range of 1×10^{10} to 1×10^{13} vg/mL.

2.19 Statistical analysis

Two-way ANOVA for repeated measures and Bonferroni/Dunn's *post hoc* test was used to compare multiple groups. Pair-wise comparison between groups was performed using the two-tailed Student's *t*-test. Data analysis was performed using the PRISM 5.0d software (GraphPad).

3. Results

3.1 Notch1 intracellular domain is acetylated in cardiomyocytes and has increased stability

We wanted to investigate whether post-translational modification of Notch1 by acetylation might modulate signalling in cardiomyocytes. We started to examine whether Notch1 was acetylated in primary neonatal rat cardiomyocytes. Three days after isolation, cells were treated with the class I and II HDAC inhibitor trichostatin A (TSA), or the class III HDAC inhibitor nicotinamide (NAM), with resveratrol, a Sirt1 activator,[35,36] with the Sirt1 inhibitor (S)-35,[37] or with the soluble form of the Notch1 ligand Jagged1 (sJ1), which we previously showed to stimulate Notch pathway in cardiomyocytes.[15] The cell lysates were fractionated into cytoplasmic and nuclear fractions and subjected to immunoprecipitation with an antibody specifically recognizing the N1ICD. Detection of the immunocomplexes with an anti-acetylated lysine antibody revealed that the N1ICD was acetylated upon sJ1 stimulation, NAM, the specific SIRT1 Inhibitor (S)-35 and, to a lesser extent, upon TSA treatment, while resveratrol abolished this effect (*Figure 1A*). Acetylation of N1-ICD was remarkably restricted to the nuclear compartment.

Next, we obtained an antibody specifically recognizing the Notch1 acetylated protein. Rabbits were immunized with peptides corresponding to three different, acetylated regions of Notch1 (Ac-Pep1, Ac-Pep2, and Ac-Pep3; Supplementary material online, *Figure S1A*), chosen according to published mass spectrometry results,[26] cf. also later. The anti-acetylated peptide antisera were tested against the corresponding peptides used for immunization and their non-acetylated versions, to evaluate specificity. Supplementary material online, *Figure S1B* shows immunoblots where scalar amounts of acetylated and non-acetylated peptides were probed with three different antisera, one corresponding to each peptide. The serum against Ac-Pep2 (ac-N1 #2B) showed specificity against the acetylated peptide and excellent sensitivity (signal in the nanogram range of the peptide). After additional purification by affinity chromatography, the three antibodies were tested in immunofluorescence experiments in HEK293 cells transfected with vectors expressing either wild type N1ICD or the N1ICD 14KR mutant.[26] We found that the ac-N1 #2B antibody only recognized the *in vivo* acetylated, wild type protein (see Supplementary material online, *Figure S1C*). Finally, the sensitivity and specificity of this antibody for acetylated Notch1 was also confirmed by western blotting using HEK293 cells transfected with wt N1ICD or the 14KR mutant. Upon cell treatment with TSA or NAM, the ac-N1 #2B antibody only recognized the wild type protein in both Notch1 immunoprecipitates and whole cell lysates (see Supplementary material online, *Figure S1D*).

We therefore used the acetylated Notch1 ac-N1 #2B antibody to re-probe the immunoprecipitated complexes in *Figure 1A*. The staining was superimposable to the results obtained using the commercial anti-acetylated lysine antibody, further supporting the nuclear localization of the acetylated N1-ICD protein.

Using the anti-acetylated Notch1 ac-N1 #2B antibody, the subcellular localization of endogenous, acetylated Notch1 protein was investigated by immunofluorescence of cultured rat cardiac myocytes, counterstained using an α-actinin antibody to specifically distinguish these cells from other cell types eventually present in the same culture. Upon treatment with both NAM, (S)-35, and TSA there was a significant increase in nuclear fluorescence. Consistent with the immunoblotting results, the same finding was also obtained after cell treatment with soluble Jagged1. Cell treatment with the γ-secrecretase inhibitor DAPT (N-[N-(3, 5-difluorophenacetyl)-L-alanyl]-S-phenylglycine t-butyl ester) markedly suppressed the staining, which is consistent with the conclusion that N1-ICD acetylation in cultured cardiomyocytes is strictly dependent on Notch1 nuclear localization (*Figure 1B*). Together, these experiments are consistent with the conclusion that activated N1ICD is acetylated in the nucleus of cardiac myocytes.

We then wanted to understand the effect of acetylation on endogenously expressed Notch1. Since Notch1 and Notch3 acetylation has been reported to regulate protein ubiquitination and degradation in other cell types,[26,38,39] we first assessed acetylation modified receptor stability in primary cardiac myocytes. We observed that Sirtuin inhibitor treatment increased both the amount and the stability of N1ICD in the

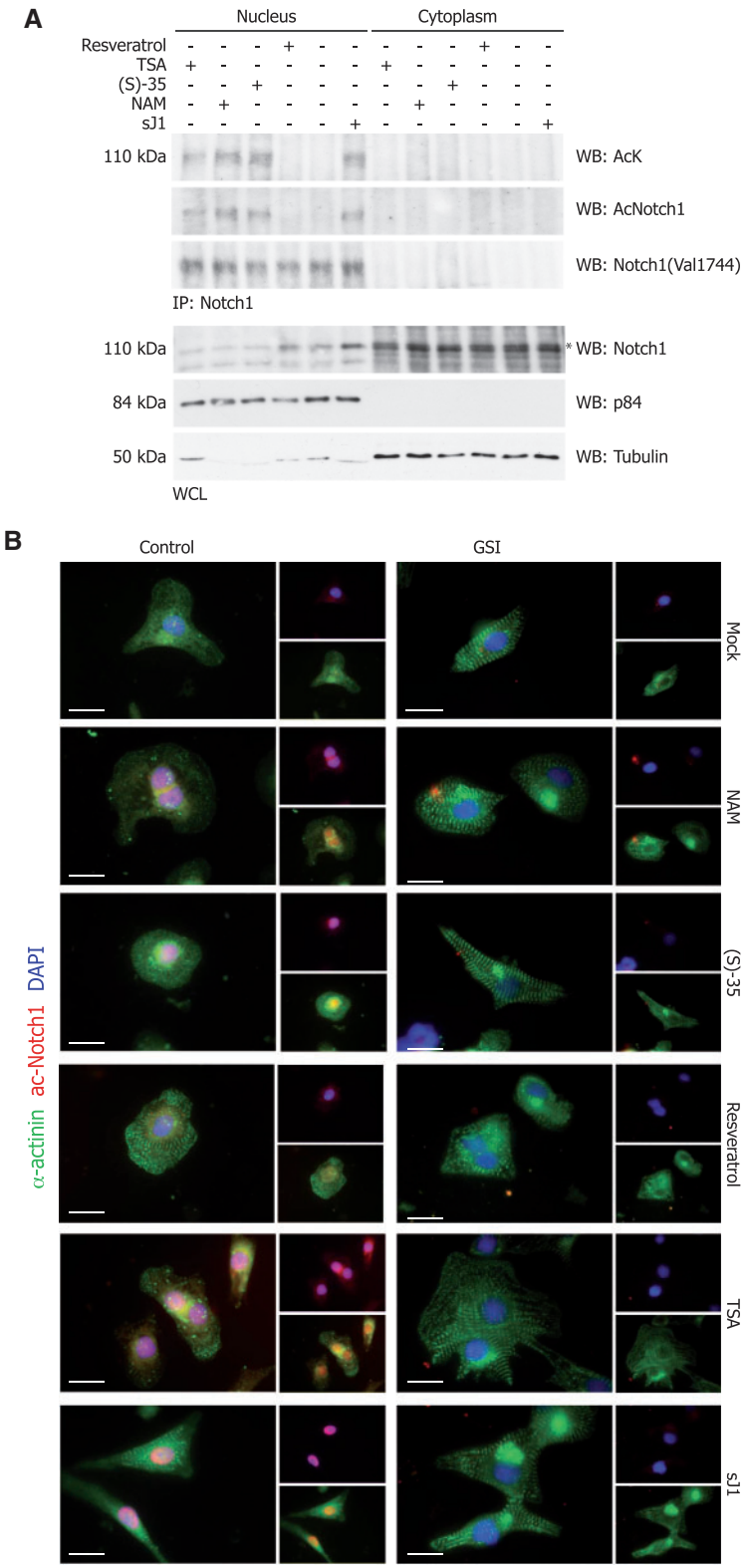

Figure 1 Notch1 intracellular domain is acetylated in cardiomyocytes and has increased stability. (*A*) Representative western blot analysis of Notch1 acetylation in primary neonatal rat cardiomyocytes, at Day 3 after isolation upon treatment with NAM (20 mM), TSA (0.5 μM), resveratrol (30 μM), (S)-35 (1 μM), or sJ1 (20×). Immunoprecipitation with an antibody against the intracellular domain of Notch1 (C20-Santa Cruz) was performed on both nuclear and cytoplasmic extracts, followed by detection with either anti-acetylated lysine, anti-acetylated N1ICD antibodies and activated Notch1 (Val1744-Cell Signalling). In the WCL, the asterisk marks the p110 band, corresponding to the active form of Notch1.The relative purity of the nuclear and cytoplasmic fractions was confirmed by sequential probing for the nuclear matrix protein p84 and the cytoplasmic marker beta-tubulin. (*B*) Subcellular localization of acetylated N1-ICD. Cardiomyocytes at Day 3 of culture were grown for 8 h in the presence of NAM (20 mM), TSA (0.5 μM) or resveratrol (30 μM),

(*Continued*)

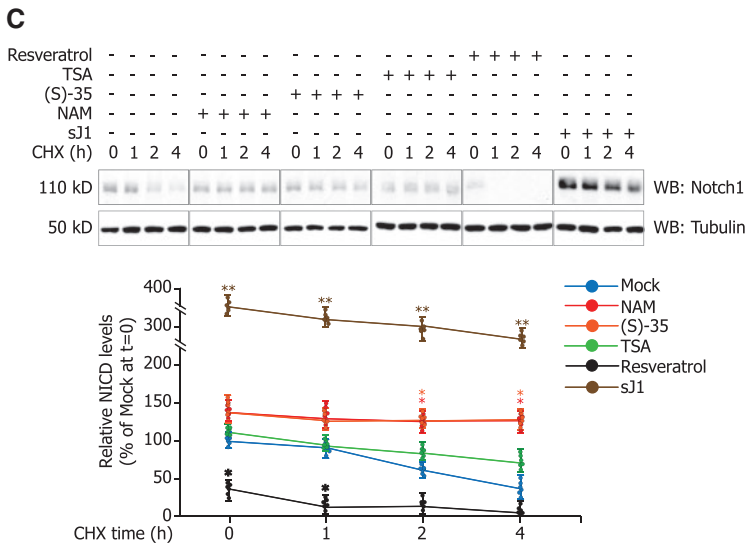

Figure 1 Continued. (S)-35 (1 μM) or sJ1 (20×). Cells were fixed and immunostained using rabbit polyclonal antibodies against acetylated Notch1 (red) and α-actinin (green); nuclei were marked with DAPI (blue). Bars: 10 μm. (*C*) Acetylation controls N1ICD stability. Representative western blot analysis showing the amounts of N1ICD in lysates from cardiomyocytes treated with NAM (20 mM), TSA (0.5 μM), resveratrol (30 μM), (S)-35 (1 μM), or sJ1 (20×), and collected at the indicated time points after addition of 10 μg/mL cycloheximide (CHX). (*D*) Quantification of the results shown in *Panel C*. The amount of N1ICD protein at time 0 was set as 100%. All values are means ± SEM ($n = 6$). *$P < 0.05$, **$P < 0.01$ vs. control, the data were analysed with one-way ANOVA and Bonferroni's multiple comparison test.

presence of the CHX, while resveratrol significantly lowered both the levels and the stability of the protein. Upon sJ1 stimulation, the total levels of the N1-ICD protein were markedly increased (*Figure 1C* and *D*). In all cases, cardiomyocyte treatment with MG132 resulted in protein stabilization (not shown; cf. also *Figure 4* later), consistent with Notch1 degradation via the proteasome. These results are consistent with the conclusion that Notch1 acetylation increases its stability by counteracting proteasomal degradation in primary cardiomyocytes.

3.2 Sirtuin inhibition enhances Notch signalling and function in cardiomyocytes

Next, we considered whether the longer intracellular half-life of acetylated Notch1 was paralleled by more robust Notch 1 transactivation activity. We assessed transcriptional activity of two Notch1-responsive promoters, the natural HES1 promoter,[40] and an artificial promoter containing four repeats of the CBF1 binding sites,[41] in both cases controlling expression of the luciferase reporter gene. Cells at Day 2 or Day 6 after isolation were transfected with either of the two luciferase reporters and treated with NAM, TSA, (S)-35, or resveratrol; transcriptional stimulation by soluble Jagged 1 served as a positive control. Consistent with the decay kinetics of the N1ICD protein, Sirt1 inhibition by both NAM and (S)-35 strongly enhanced the activation of both the HES1 and CBF reporters in cells analysed at Day 3 after isolation (*Figure 2A* and Supplementary material online, *Figure S2A*, respectively). In contrast, resveratrol decreased the transcriptional response. The same qualitative response was also detected in cells transfected at Day 6 after isolation, however the magnitude of transcriptional activation was significantly blunted (*Figure 2B* and Supplementary material online, *Figure S2B*, respectively), according with a decrease in Hes1 expression levels (see Supplementary material online, *Figure S3*). Notch-1 signalling inhibition by cell treatment with DAPT markedly suppressed promoter activation in all the experimental settings ($P < 0.001$ in all conditions). These results are consistent with the conclusion that both Hes1 and CBF-1 reporter activation in cultured cardiomyocytes are strictly dependent on Notch1 acetylation.

To assess whether the modulation of Notch1 acetylation by sirtuin activation or inhibition might impact on cardiomyocyte proliferation, the levels of incorporation of the thymidine analogue EdU were analysed at Days 3 and 7 after isolation. Resveratrol markedly decreased the number of EdU^+ cardiomyocytes at both Days 3 and 7 of culture. In contrast, both NAM and the Sirt1 inhibitor (S)-35 significantly increased the number of proliferating cardiomyocytes (*Figure 2C* and *D*); Jagged1 stimulation served as a positive control in these experiments. Treatment with DAPT determined a marked decrease in the number of EdU-positive cardiomyocytes in all conditions. Representative images of these experiments are shown in *Figure 2E*.

Modulation of acetylation by sirtuin stimulation or inhibition also impacted on Notch regulation of cardiomyocyte apoptosis. Both NAM and (S)-35 treatment of cultured cardiomyocytes significantly decreased the number of apoptotic cells at both Days 3 and 7, as assessed by a caspase assay, to an extent comparable to soluble Jagged1 stimulation; resveratrol also had a robust protective effect in this assay, consistent with previously findings.[42] In contrast, blocking the proteolytic processing of Notch1 with DAPT markedly increased the number of apoptotic cells at both Days 3 and 7 of culture (*Figure 2F* and *G*). Notably, the induction of apoptosis upon γ-secretase inhibition was less profound at the later time point, consistent with our previous observations.[15]

Together, these experiments indicate that the regulation of Notch1 acetylation by sirtuins modulates the biological functions of Notch1 in primary cardiomyocytes.

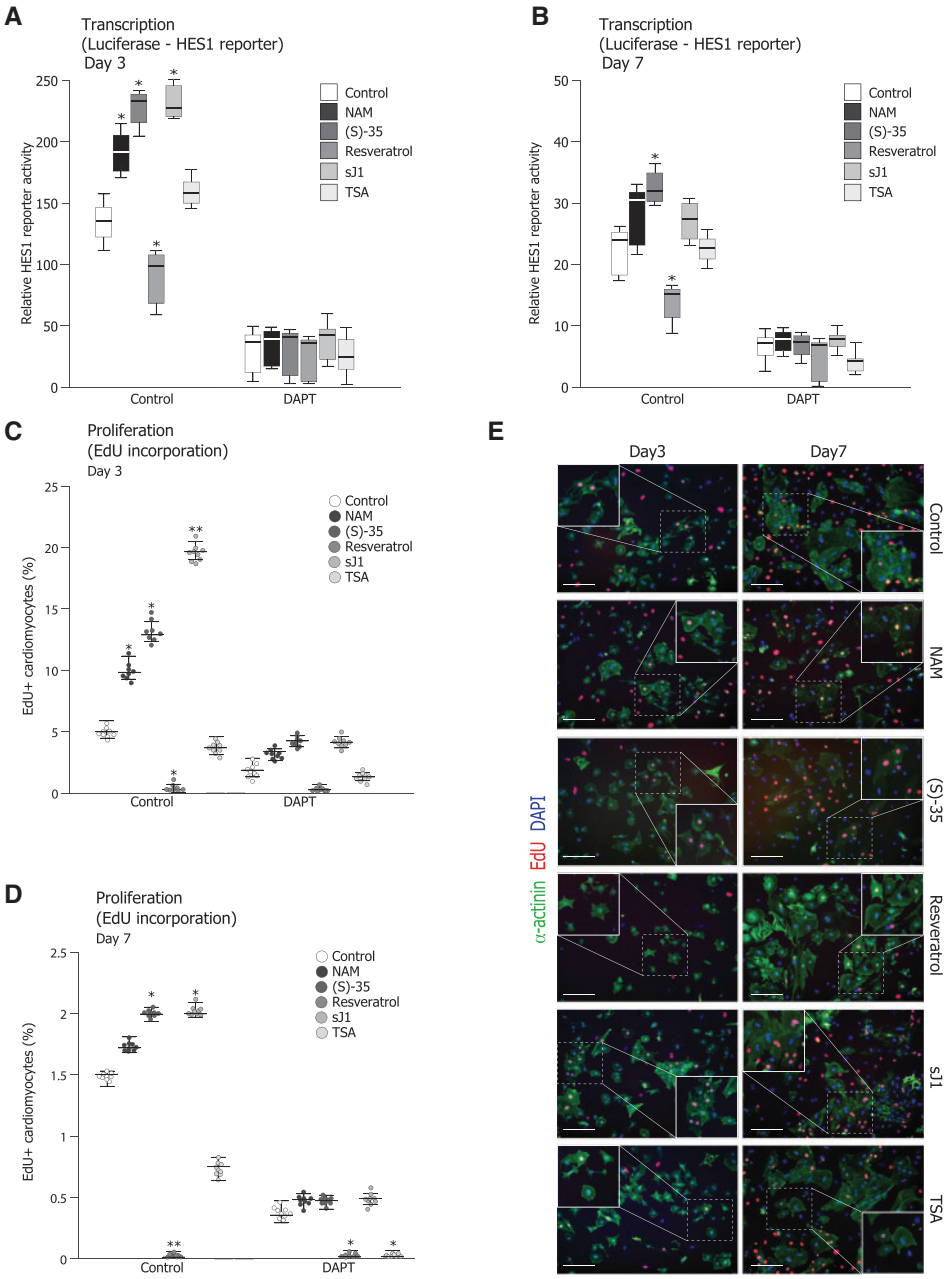

Figure 2 Sirtuin inhibition enhances Notch signalling and function in cardiomyocytes. Sirt1 inhibition enhances HES1-luciferase reporter transcription. Cardiomyocytes at Day 2 or Day 6 after isolation were transfected with 0.5 μg of HES1 (*A* and *B*) firefly luciferase reporter and 0.01 μg of a Renilla luciferase reporter before treatment with NAM (20 mM), TSA (0.5 μM), resveratrol (30 μM), (S)-35 (1 μM), or sJ1 (20×) for 8 h in DMSO-(Control) or DAPT containing medium (γ-secretase inhibitor, 20 μM); luciferase activity was measured 24 h later. Firefly luciferase activity was normalized using Renilla luciferase activity. Transcriptional stimulation by soluble Jagged 1 served as a positive control; DAPT treatment markedly suppressed HES1-luciferase reporter activation. The transactivation effect was evaluated at the indicated time points (Day 3 *Panel A*; Day 7 *Panel B*). The histograms show mean ± SEM; $n = 7$ (four replicates/independent experiment). $^{*}P < 0.05$, $^{**}P < 0.01$, vs. control. The data were analysed with one-way ANOVA and Bonferroni's multiple comparison test (*C* and *D*) Resveratrol inhibits cardiomyocytes proliferation. Neonatal cardiomyocytes after 2 or 6 days of *in vitro* culture, were grown for 8 h in the presence of NAM, (S)-35, TSA, resveratrol, or sJ1, in DMSO-(Control) or DAPT containing medium (20 μM). After pulse-labelling with EdU and specific detection, the total number of EdU+ cardiomyocytes was evaluated. DAPT blocked cardiomyocyte proliferation in any tested condition. The graphs show mean ± SEM; $n = 9$ (four replicates/independent experiment); $^{*}P < 0.05$; $^{**}P < 0.01$ vs. control. The data were analysed with one-way ANOVA and Bonferroni's multiple comparison test. (*E*) Representative images of EdU+ cardiomyocytes (Day 3 and 7 of culture); sJ1 was used as a positive control for Notch1 activation. Green, α-actinin; red, EdU-positive nuclei; blue, DNA (DAPI). Bar, 100 μm. Magnifications of the boxed areas are shown in the insets. (*F* and *G*) Caspase assay was performed on neonatal cardiac myocytes grown for 8 h in the presence of NAM, (S)-35, TSA, resveratrol or sJ1 in DMSO-(Control) or DAPT containing medium (20 μM), after 3 or 7 days of *in vitro* culture; stimulation by soluble Jagged 1 was used as a positive control. The inhibition of Notch1 processing by DAPT markedly increases cardiomyocyte apoptosis through a specific Notch-dependent pathway. All values are means ± SEM ($n = 9$, four replicates/independent experiment), $^{**}P < 0.01$ vs. control. The data were analysed with one-way ANOVA and Bonferroni's multiple comparison test.

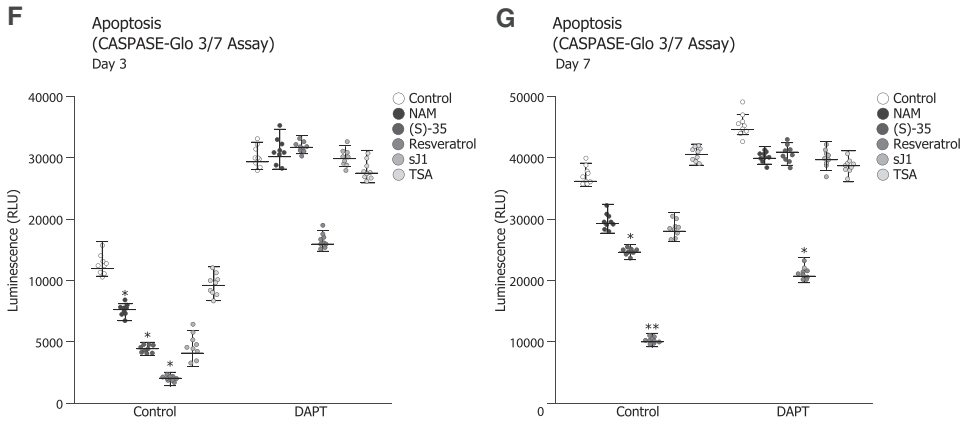

Figure 2 Continued.

3.3 Modulation of Notch1 stability by AAV-mediated gene transfer in primary cardiomyocytes

Gene transfer and persistent transgene expression in primary cardiac myocytes can be efficiently achieved using viral vectors based on the Adeno-Associated Virus serotype 6 (AAV6).[43] To further unravel the biological relevance of Notch1 acetylation in cardiac myocytes, we generated AAV6 vectors expressing the myc-tagged N1ICD or its isoform devoid of the PEST domain [N1ICD(ΔC); *Figure 3A* and *B, Panel a*]. Neonatal rat ventricular cardiomyocytes were transduced with either of the two vectors (MOI = 5×10^3 vg/cell); 72 h after infection, cells were treated with NAM, (S)-35, TSA, or resveratrol. Immunodetection of virally transduced N1ICD in cell lysates using an anti-acetylated lysine antibody revealed an acetylation response superimposable to that of the endogenous protein. In contrast, the N1ICD(ΔC) mutant was also found acetylated in untreated and resveratrol-treated cells [*Figure 3* and *B, Panel b*, for N1ICD and N1ICD(ΔC) respectively].

Next, we wanted to assess the stability of the two transduced proteins. After CHX treatment, N1ICD showed a decay rate and drug sensitivity comparable to that of the endogenous receptor, while N1ICD(ΔC) was significantly more stable even in the absence of the HDAC inhibitors, consistent with the absence of the protein PEST domain (*Figure 3A* and *B, Panel c*). In all conditions, blocking the proteasome by cell treatment with MG132 increased the protein levels, consistent with protein decay through proteasomal degradation.

The experiments so far described underline the role of Notch 1 acetylation in increasing stability of the protein. We therefore wanted to test whether a constitutively acetylated form of Notch1 might be intrinsically more stable. For this purpose, we exploited a genetic strategy used to increase acetylation of human immunodeficiency virus-1 (HIV-1) integrase,[44] consisting in the in-frame fusion of the p300 acetyltransferase catalytic domain at the C-terminus of N1ICD(ΔC), to generate N1ICD(ΔC)-HAT; (*Figure 3C, Panel a*). After cardiomyocyte transduction (MOI = 5×10^3 vg/cell), we found that this protein was more acetylated than N1ICD, even in the absence of drug treatment (compare *Panel b* in *Figure 3A* and *C*). This constitutively acetylated fusion protein was remarkably more stable over time after CHX treatment even in the presence of resveratrol (*Figure 3C, Panel c*). As a control, we also obtained a mutant construct, carrying an inactivating mutation in the p300 acetyltransferase catalytic site [N1ICD(ΔC)-D1395YHAT].[45] We found that this mutant was essentially not acetylated even in the presence of NAM or TSA (see Supplementary material online, *Figure S4A*).

Subsequently, we also wanted to determine which lysines were acetylated in the HAT-fusion Notch1 protein. For this purpose, we transfected this construct in HEK293T cells and analysed acetylation by MALDI-TOF/TOF mass spectrometry. Three independent analyses revealed the presence of 18 acetylated lysine residues, including those recognized by our anti-acetylated Notch1 #2B antibody (aa. 2144-2167; Supplementary material online, *Figure S4B*).

Finally, we also generated an AAV6 vector coding for Sirt1 (*Figure 3D, Panel a*) and tested its effect after transduction of neonatal cardiomyocytes (MOI = 5×10^3 vg/cell) in the presence of NAM, (S)-35, TSA, or resveratrol; stimulation with sJ1 was used as a positive control. Expression of Sirt1 significantly decreased the levels of endogenous N1ICD acetylation, which was maintained in cells treated with the Sirt1 chemical inhibitors NAM- and (S)-35. Consistently, the levels of Notch1 protein in total cell lysates was decreased in AAV6-SIRT1-transduced cardiomyocytes, unless Sirt1 was inhibited (*Figure 3D, Panel b*). The reduction in Notch1 protein was not due to a decrease in gene transcription, since the levels of its mRNA were unchanged in transduced cells, while those of one of its main targets (Hes1) were significantly decreased (see Supplementary material online, *Figure S5*). Consistent with an effect of AAV6-SIRT1 on protein stability, cell treatment with MG132 restored Notch1 levels (*Figure 3D, Panel c*).

Together, these results reinforce the conclusion that acetylation is an essential determinant of Notch1 levels and indicate that Sirt1, by counteracting this modification, negative regulates the stability of the protein in primary cardiomyocytes.

3.4 Acetylation regulates Notch1 intracellular signalling and enhances the proliferative potential of neonatal rat cardiomyocytes

Next, we assessed the functional effect of AAV6-N1ICD, AAV6-N1ICD(ΔC), N1ICD(ΔC)-HAT, and AAV6-SIRT1 on Notch1 downstream signalling in neonatal rat cardiac myocytes. The experiments

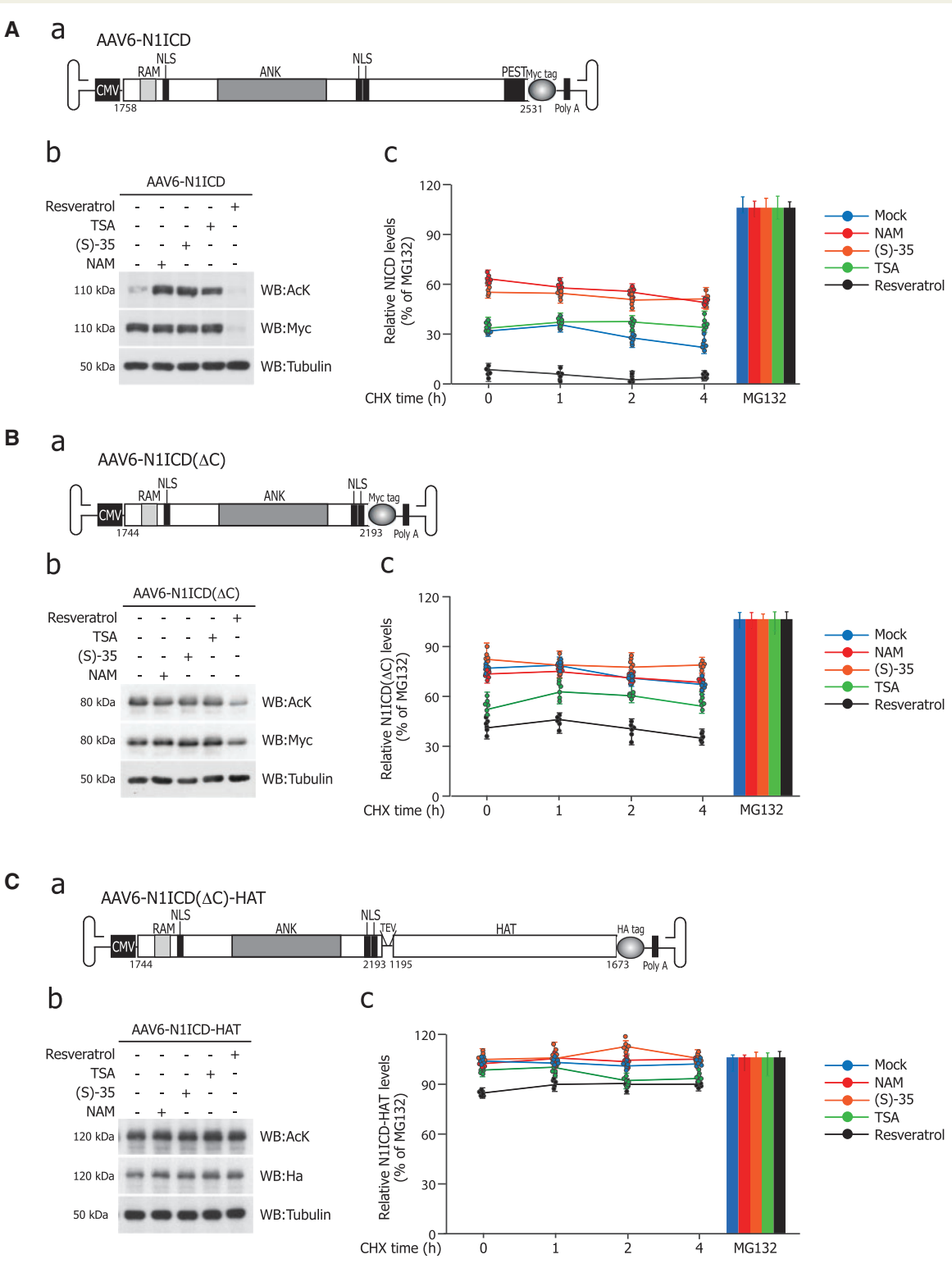

Figure 3 Modulation of Notch1 stability by AAV-mediated gene transfer in primary cardiomyocytes. (*A*, *Panel a*) Schematic representation of AAV6-N1ICD vector with the indication of the main Notch functional domains (CMV, cytomegalovirus immediate-early promoter; RAM, RBPj-associated molecule; ANK, ankyrin repeats; NLS, nuclear localization signal; PEST, proline (P), glutamic acid (E), serine (S), and threonine (T) enriched sequence; Poly-A, polyadenylation site; numbering is according to the Notch1 mouse protein). (*Panel b*) Neonatal rat cardiomyocytes were transduced with the AAV6-N1ICD vector (MOI = 5×10^3 vg/cell) and, 2 days after transduction, treated for 8 h with 20 mM NAM, 0.5 μM TSA, 1 μM (S)-35,or 30 μM resveratrol. The picture shows a representative western blotting with the indicated antibodies (AcK, anti-total lysine antibody; Myc, 9E10, anti Myc-tag antibody).

(*Continued*)

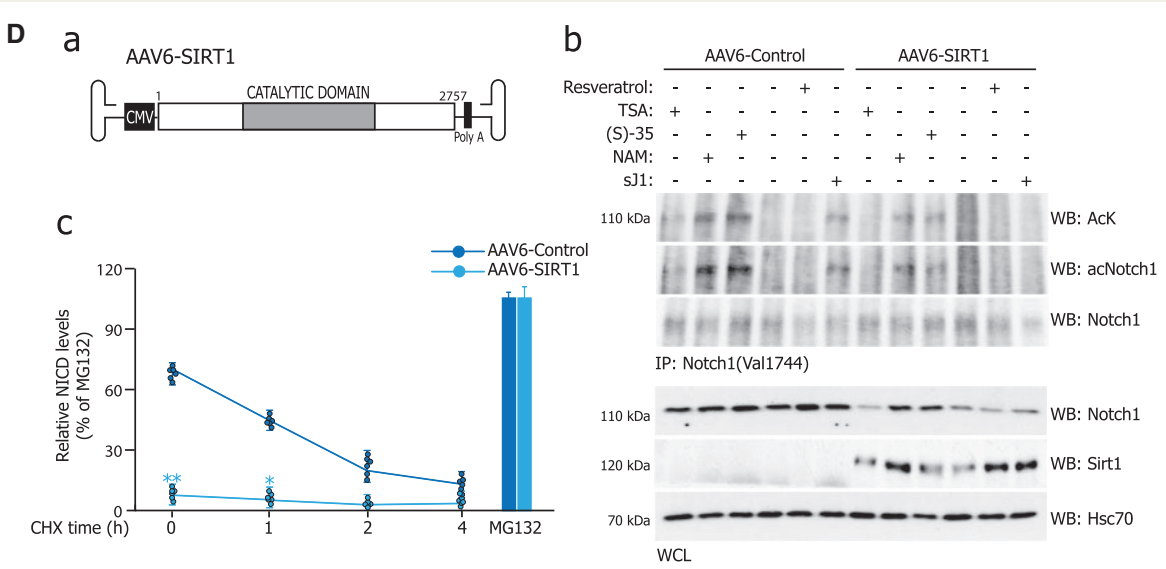

Figure 3 Continued. (*Panel c*) Relative quantification of the amounts of AAV6-N1ICD protein in transduced neonatal cardiomyocyte lysates, collected at the indicated time points after addition of 10 μg/mL cycloheximide (CHX), treated with either NAM, (S)-35, TSA, or resveratrol. In the graphs, the amount of protein was set at 100% in samples treated for 4 h in the presence of the proteasome inhibitor MG132 (10 μM-histograms). The results are expressed as the mean average deviations of six independent experiments; bars indicate mean ± SD; $^{*}P < 0.05$; $^{**}P < 0.01$. The data were analysed with one-way ANOVA and Bonferroni's multiple comparison test. (B, *Panels a–c*) Same as in *Panel A* for the AAV6-N1ICD(ΔC) vector, deleted of the C-terminal 338 amino acids, which include the PEST domain. (*C, Panels a–c*) Same as in *Panel A* for the AAV6-N1ICD(ΔC)-HAT vector, carrying a C-terminal extension corresponding to the p300 catalytic domain. (*D, Panel a*) Schematic representation of AAV6-SIRT1 vector; the grey box indicates the conserved catalytic core domain of the protein. (*Panel b*) Western blot analysis of Notch1 acetylation in cardiomyocytes, after AAV-driven overexpression of Sirt1. Freshly isolated neonatal rat cardiomyocytes were transduced with the AAV6-SIRT1 vector (MOI = 5×10^3 vg/cell) and, 3 days after transduction, treated with NAM, (S)-35, TSA or resveratrol. sJ1 (20×) was used as a positive control. Immunoprecipitation with an antibody specifically recognizing the activated form of Notch1 (Val 1744) was followed by detection either with anti-acetylated lysine or anti-acetylated N1ICD antibodies. (*Panel c*) SIRT1 decreases the stability of N1ICD in transduced cardiomyocytes. Relative quantification of the amounts of N1ICD in lysates from cardiomyocytes transduced with a control vector or AAV6-SIRT1, collected at the indicated time points after addition of 10 μg/ml cycloheximide (CHX). In the graphs, the amount of proteins was set at 100% in samples maintained 4 h in the presence of the proteasome inhibitor MG132 (10 μM-histograms). Results are expressed as mean ± SD of five separate experiments. $^{*}P < 0.05$. The data were analysed with one-way ANOVA and Bonferroni's multiple comparison test.

were performed by transfecting the reporter plasmids in which luciferase expression is controlled by the HES1 and CBF1 promoter into cardiomyocytes transduced with each of the four vectors, followed by the measurement of gene expression at Days 3 and 7. Cell treatment with the γ-secretase inhibitor DAPT served to block the endogenously expressed Notch1 receptor signalling. The results of these experiments are shown in Supplementary material online, *Figure S5A–D*. Parallel to the acetylation profile and consistent with the decay kinetics, both AAV6-N1ICD and AAV6-N1ICD(ΔC) triggered a strong activation of both reporters in both Day 3 and 7 cardiomyocytes; the latter vector was significantly more effective, in keeping with the increased stability of the encoded protein. Of interest, while AAV6-SIRT1 did not show any appreciable transcriptional effect, the constitutively acetylated N1ICD(ΔC)-HAT construct was remarkably effective in activating of downstream Notch signalling, triggering a strong activation of both reporters at both Days 3 and 7. DAPT did not affect the transactivation effect driven by any of the N1ICD mutants.

To assess the role of Notch1 acetylation in the modulation of cardiomyocyte proliferation, we transduced neonatal rat cardiomyocytes with each of the four AAV6 vectors (MOI = 5×10^3 vg/cell), followed by the analysis of BrdU incorporation at 3, 7, and 12 days after a single 24 h-pulse prior to cell fixation; transgene expression was sustained at all time points (see Supplementary material online, *Figure S7*). The proteasome resistant AAV6-N1ICD(ΔC) and the stably acetylated AAV6-N1ICD(ΔC)-HAT proteins increased the number of BrdU$^+$, α-actinin$^+$ cells at Day 3 [18% and 17.5% of proliferating cells transduced with AAV6-N1ICD(ΔC) and AAV6-N1ICD(ΔC)-HAT, respectively, compared with 13% detected in cells infected with a control vector]. The full length Notch1 isoform (AAV6-N1ICD) was less effective, while the AAV6-SIRT1 vector did not exert any recordable proliferative effect (*Figure 4A* and *B* for quantification and representative images, respectively). The strongest effect of stimulation of cardiomyocyte proliferation was obtained at later time points. After 7 days of culture, 17% and 17.5% of cardiomyocytes infected with AAV6-N1ICD and AAV6-N1ICD(ΔC), respectively, scored positive for BrdU incorporation, and this percentage rose to 21% in the cells transduced with AAV6-N1ICD(ΔC)-HAT; these numbers have to be compared with the 6% of BrdU$^+$ cells observed in cardiomyocytes transduced with a control AAV6 vector (*Figure 4A* and *C*). After 12 days of culture, proliferation in control infected cells was almost extinguished (approximately 2% BrdU$^+$ cardiomyocytes), while transduction with both AAV6-N1ICD and AAV6-N1ICD(ΔC) caused a residual proliferative effect (approximately 5.2% and 6%,

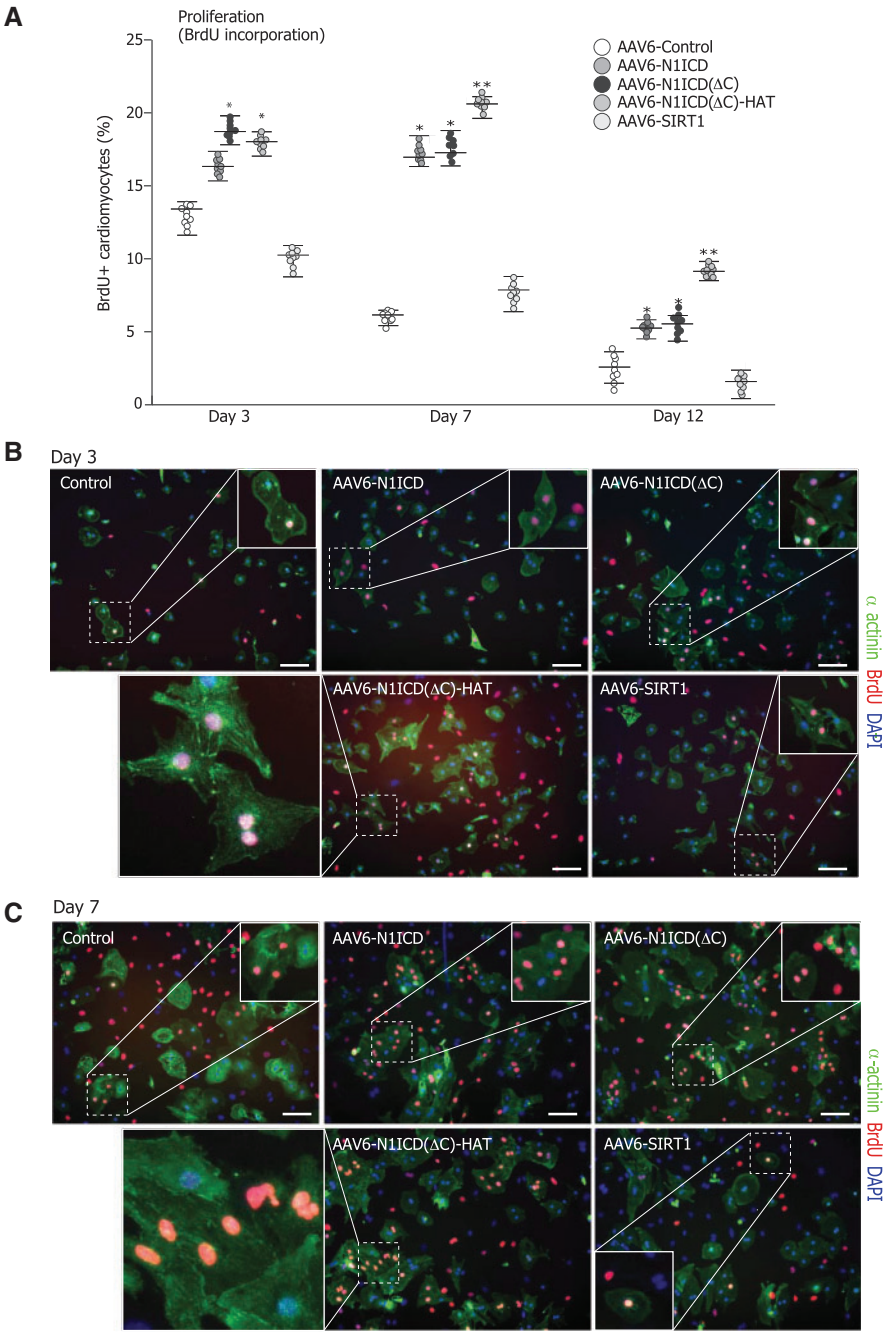

Figure 4 Acetylation of N1ICD enhances BrdU incorporation of neonatal rat cardiomyocytes. (*A*) Freshly isolated rat neonatal cardiomyocytes were transduced with AAV6-MCS (Control), AAV6-N1ICD, AAV6-N1ICD(ΔC), N1ICD(ΔC)-HAT, or AAV6-SIRT1 (MOI = 5×10^3 vg/cell). After 3, 7 or 12 days of *in vitro* culture, the total number of α-actinin$^+$/BrdU$^+$ cells was evaluated. Results are representative of 7–9 independent experiments (four replicates/independent experiment); at the indicated time points; shown are mean ± SEM; *$P < 0.05$; **$P < 0.001$ vs. AAV-MCS. The data were analysed with one-way ANOVA and Bonferroni's multiple comparison test. (*B*–*D*) Representative images of BrdU$^+$ cardiomyocytes after the AAV-mediated gene transfer (Day 3, 7, and 12 of culture, respectively). The images are representative of seven independent experiments, (five replicates/independent experiment). Magnifications of the boxed areas are shown in the insets. Arrows point at BrdU+ nuclei. Green, α-actinin; red, BrdU; blue, DNA (DAPI). Scale bars: 50 μm.

respectively; *Figure 4A* and *D*). Again, AAV6-N1ICD(ΔC)-HAT was the most effective vector, determining the appearance of approximately 10% of BrdU$^+$ cells; notably, the formation of clusters of BrdU$^+$ cardiomyocytes was readily appreciable, with few mitotic figures visible on the plate (*Figure 4D*). AAV6-SIRT1 failed to stimulate cardiomyocyte proliferation in any of the tested conditions. The effect of AAV6-N1ICD, AAV6-N1ICD(ΔC), and N1ICD(ΔC)-HAT was independent from the endogenous Notch1 receptor, since their effect on BrdU incorporation was insensitive to DAPT treatment at any time point (see Supplementary material online, *Figure S8*).

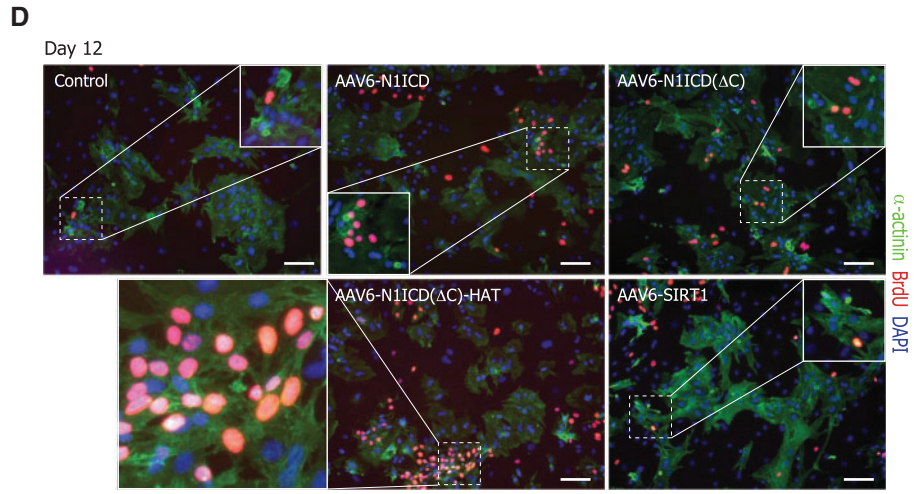

Figure 4 Continued.

To demonstrate that the increase in proliferation eventually resulted in an increase in karyokinesis and cytokinesis, we also evaluated positivity for histone H3-serine10 phosphorylation [pH3(S10), a marker of mitosis; *Figure 5A* and *B* for quantification and representative images at Day 3, respectively] and for localization of AuroraB kinase in midbodies (showing cytokinesis; *Figure 5C* and *D*). Transduction with AAV6-N1ICD, AAV6-N1ICD(ΔC), and N1ICD(ΔC)-HAT significantly increased both the percentage of cells positive for H3S10ph (3.7%, 4%, and 5% respectively, compared to 3% of control cells), and the number of cells presenting midbodies (1.6%, 1.4%, and 2%, respectively, compared to 0.8%). Notably, the effect was more evident after 1-week of culture, when both AAV6-N1ICD, AAV6-N1ICD(ΔC), and N1ICD(ΔC)-HAT triggered a significant increase in the positivity for H3S10ph and for Aurora B kinase localization in midbodies, compared to both control and AAV6-Sirt1-transduced cardiomyocytes. Of interest, AAV6-N1ICD(ΔC)-HAT still exerted a significant effect on transduced cardiomyocytes even after 12 days of culture. Taken together, these results indicate that the proliferative capacity of neonatal cardiomyocytes correlates with the activation of Notch signalling and, in particular, that Notch1 acetylation acts as a rheostat to positively tune proliferation.

3.5 Acetylation of N1ICD enhances the regenerative response in neonatal mice upon heart apical resection

The mammalian heart retains a transient capacity for cardiac regeneration during fetal and early neonatal life. In this time frame, Notch1 is expressed in heart tissue and regulates cardiomyocyte proliferation upon injury.[19,46] To assess whether acetylation of N1ICD impacts myocardial regeneration in vivo, we surgically resected the left ventricular apex leading to exposure of the ventricle chamber (~15–20% of the ventricular myocardium) in mice immediately after birth[30]; the day after surgery, we transduced both sham and operated mice with either AAV9-Control, AAV9-N1ICD, AAV9-N1ICD(ΔC), or N1ICD(ΔC)-HAT ($n = 6$ per group). We then analysed the regenerative response 7 and 21 days after surgery (*Figure 6A*). In all animals, histological analysis revealed progressive regeneration of the apex, with gradual resorption of the apical scar (*Figure 6B*, *Panels a-d-g-l*), its replacement by α-actinin+ myocardial tissue and restoration of the resected myocardium within 21 days (*Figure 7A*, *Panels a-d-g-l*). The regeneration process was accompanied by a wave of cardiomyocyte proliferation: in AAV-Control animals 7 days after surgery, 9.2% of cardiac myocytes scored positive for BrdU (vs. 7.4% of sham animals) and 4.0% was progressing into mitosis, as assessed by pH3(S10)+ positivity, compared to 1.9% of sham animals (*Figure 6D, E* and *B*, *Panels b and c* and *C*, *Panels b and c* for quantification and representative images, respectively). The proliferative response was exhausted 3 weeks after surgery, resulting in 3.3% of BrdU+ cardiac myocytes, vs. 2.3% of sham) and <1% of pH3(S10)+ (vs. 0.1% of sham) cardiomyocytes at Day 21 (*Figure 7C, D* and *A*, *Panels b and c* and *B*, *Panels b and c* for quantification and representative images, respectively).

To specifically evaluate the contribution of the expressed transgenes to the regeneration process, we analysed the proliferative response of cardiac myocytes both in sham and resected mice transduced with the vectors at Days 7 and 21 after surgery. For all vectors, transgene expression was sustained at all time points (see Supplementary material online, *Figure S9*). The proteasome-resistant AAV9-N1ICD(ΔC) and the stably acetylated AAV9-N1ICD(ΔC)-HAT proteins increased the number of BrdU+, α-actinin+ cells (19.7% and 21.1% of proliferating cells, respectively, compared to 7.4% in hearts transduced with a control vector). The full length Notch1-ICD isoform (AAV9-N1ICD) was less effective (13.1%), putatively due to its shorter half life (*Figure 6D* and *B*, *Panels b-e-h-m* for quantification and representative images, respectively). The increase in BrdU incorporation driven by the transgenes was paralleled by an increase of pH3(S10)+ cardiomyocytes [7.4% and 8.25% after transduction with AAV9-N1ICD and AAV9-N1ICD(ΔC), respectively]. This percentage rose to approximately 10% in hearts transduced with AAV9-N1ICD(ΔC)-HAT, vs. 2% in the control vector (*Figure 6E* and *B*, *Panels b-e-h-m* for quantification and representative images, respectively). The strongest effect was evident 3 weeks after surgery. At this time point, proliferation in control infected cells was almost extinguished (approximately 2% BrdU+ cardiomyocytes), while transduction with both AAV9-N1ICD and AAV9-N1ICD(ΔC) resulted in a longer lasting proliferative effect (approximately 4.3% and 8.8% BrdU+ cardiomyocytes, respectively; *Figure 7B*, *Panels e–h*; *C* for quantification). Again,

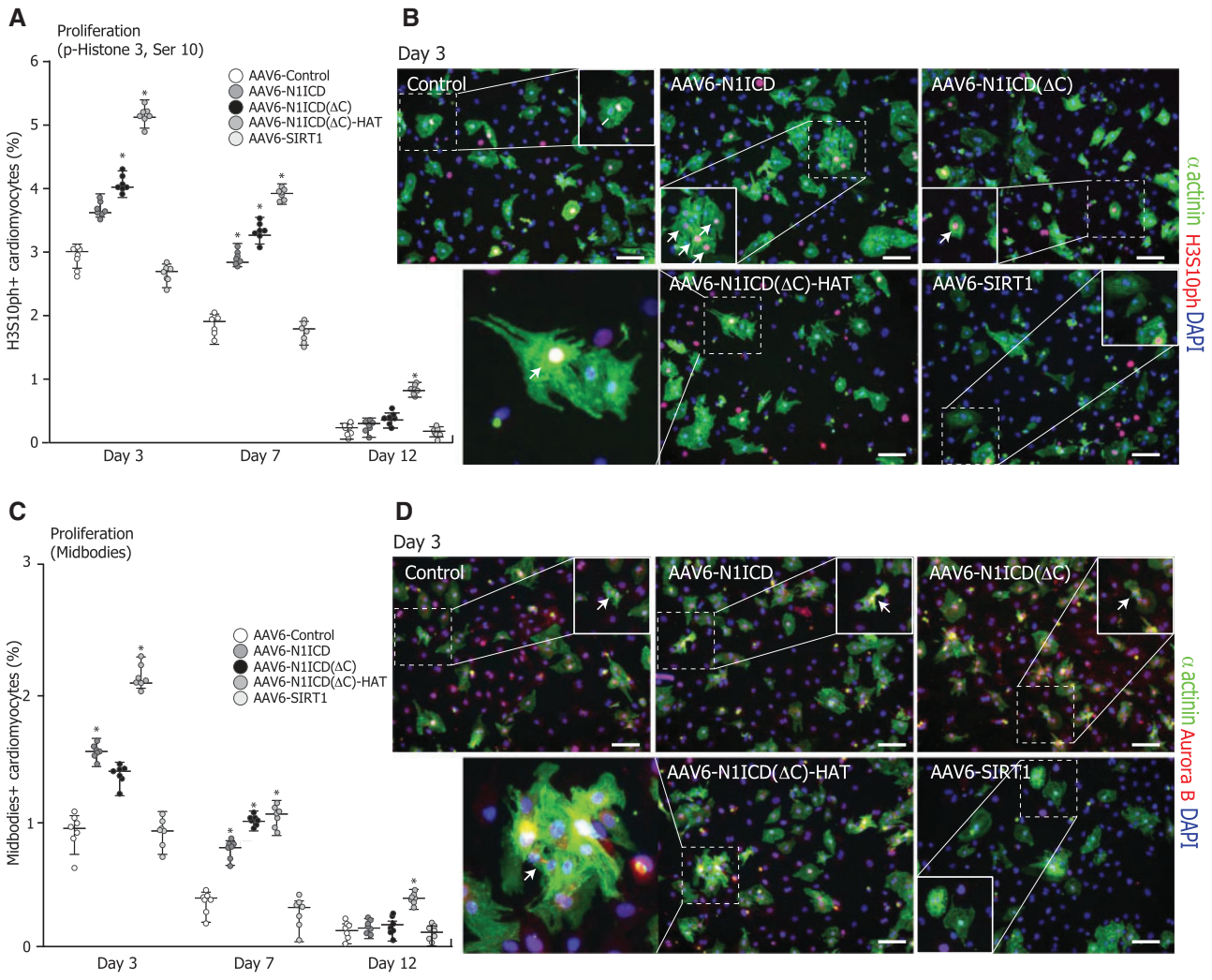

Figure 5 Acetylation of N1ICD enhances the proliferative potential of neonatal rat cardiomyocytes. (*A*) Freshly isolated rat neonatal cardiomyocytes were transduced with AAV6-MCS (Control), AAV6-N1ICD, AAV6-N1ICD(ΔC), N1ICD(ΔC)-HAT, or AAV6-SIRT1 (MOI = 5×10^3 vg/cell). After 3, 7, or 12 days of *in vitro* culture, the total number of α-actinin$^+$/phospho-histone H3, Ser 10$^+$ cells (mitotic cardiomyocytes) was evaluated. Results are representative of seven independent experiments (five replicates/independent experiment); at the indicated time points; shown are mean ± SEM; *$P < 0.05$; **$P < 0.001$ vs. AAV-MCS. Data are means ± SD, two-way ANOVA, Bonferroni's multiple comparison test. (*C*) Same as in *Panel A* for Aurora B kinase present in midbodies; (*B–D*) Representative images of pHis3$^+$ (*B*) and AuroraB$^+$ (*D*) cardiomyocytes after the AAV-mediated gene transfer. Magnifications of the boxed areas are shown in the insets. Arrows point at pHis3$^+$ and and AuroraB$^+$ cardiomyocytes. Green, α-actinin; red, pHis3 (*B*) and AuroraB (*D*); blue, DNA (DAPI). Scale bars: 50 μm.

AAV9-N1ICD(ΔC)-HAT was the most effective, determining the appearance of more than 10% of BrdU+ cells (*Figure 7B, Panel m*). The effect on DNA synthesis was paralleled by an increase in pH3(S10) positivity, which raised from 1.7% in the case of AAV9-N1ICD, to 3.75 and 4.7% in the cases of AAV9-N1ICD(ΔC) and AAV9-N1ICD(ΔC)-HAT, respectively (*Figure 7B, Panels f-i-n* and *D* for quantification). These findings confirm the capacity of Notch1 of sustaining the proliferation of cardiac cells in neonatal mice, keeping their proliferative window open for a longer time.

The most relevant effect of the in vivo delivery of acetylated Notch1 was upon apex surgical resection. In vivo transduction of AAV9-N1ICD, AAV9-N1ICD(ΔC) or AAV9-N1ICD(ΔC)-HAT increased the number of cycling cardiomyocytes. One week after surgery, ~18% of cardiomyocytes scored positive for BrdU in AAV9-N1ICD-transduced animals and more than 24% in mice transduced with AAV9-N1ICD(ΔC) and AAV9-N1ICD(ΔC)-HAT (to be compared with ~9% of control animals) (*Figure 6B, Panels e-h-m* and *D* for quantification). These results were mirrored by pH3(S10) staining: all the three vectors increased the number of pH3(S10)+ cardiomyocytes after apical resection, which raised from ~4% in control animals to ~10% in the cases of both AAV9-N1ICD and AAV9-N1ICD(ΔC) transduction, to reach 11.5% for AAV9-N1ICD(ΔC) (*Figure 6B, Panels f-i-n* and *E* for quantification). The last vector determined its strongest effect in resected animals 21 days after surgery. At this time point, the scar caused by the tissue resection was almost completely resorbed in most animals (*Figure 7A, Panels a-d-g-l*) and the endogenous proliferation of cardiomyocytes in Control animals

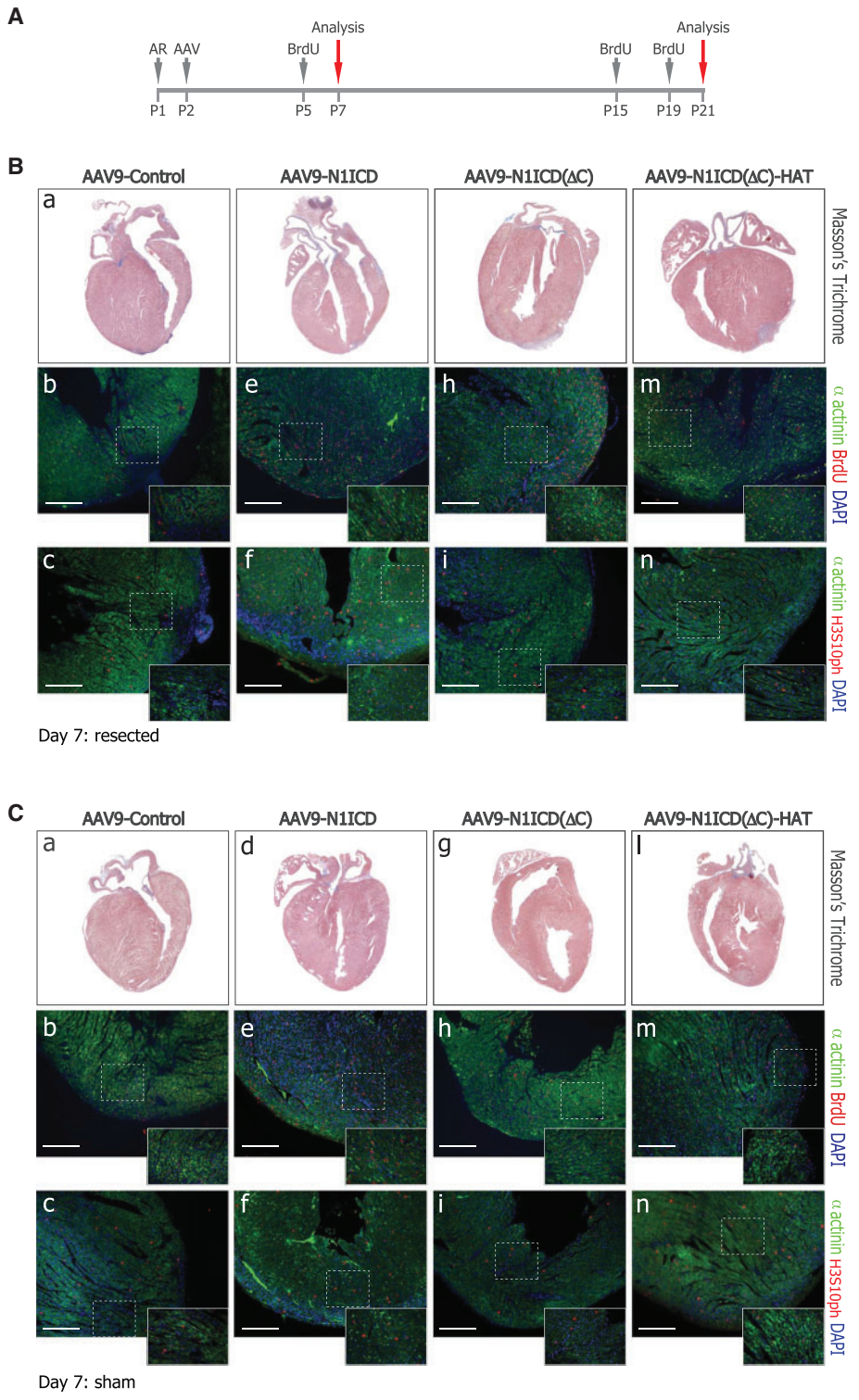

Figure 6 Acetylation of N1ICD sustains the regenerative potential of hearts after apical resection. (*A*) Schematic representation of the time course of the *in vivo* experiments; AR, apical resection; AAV, Adeno-Associate Vector transduction; BrdU, Bromodeoxyuridine. (*B*). Representative images of resected hearts from mice transduced with AAV9-MCS (Control), AAV9-N1ICD, AAV9-N1ICD(ΔC), N1ICD(ΔC)-HAT 7 days after surgery. (*Panels a-d-g-l*) Histology of resected hearts 7 days after surgery and AAV transduction. Azan-Mallory trichrome staining of representative cross-sections of one heart/group ($n = 6$ per group). (*Panels b-e-h-m*) Representative images of BrdU+ cardiomyocytes in resected animals at Day 7 after surgery and AAV-mediated gene transfer. (blue: Dapi; green: α actinin; red: BrdU; scale bar: 100 μm), quantification in *D*. (*Panels c-f-i-n*) Representative images of pH3-Ser10+ cardiomyocytes in resected animals at Day 7 after surgery and AAV-mediated gene transfer (blue: Dapi; green: α-actinin; red: phosho-H3Ser10; scale bar: 100 μM), quantification in *E*. (*C*). Same as in *Panel B* for Sham operated mice. (*D*). Quantification of of BrdU+ cardiomyocytes in sham and resected animals at Day 7 after surgery and AAV-mediated gene transfer. Data are mean ± SEM; $n = 6$ per group; two-way ANOVA, Bonferroni's multiple comparison test; $^{*}P < 0.05$, $^{**}P < 0.01$, $^{***}P < 0.001$ relative to AAV-MCS transduced animals, used as a control. S, Sham; R, Resected animals. (*E*) Same as in *Panel D* for phosho-H3Ser10+ cardiomyocytes.

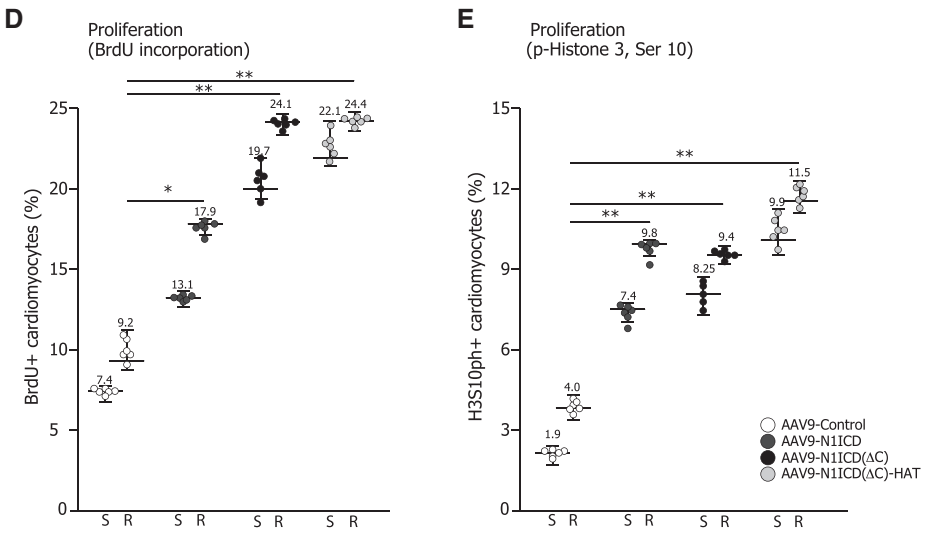

Figure 6 Continued.

was virtually exhausted (∼3% of BrdU+ and ∼1% of pH3(S10)+ cardiomyocytes, *Figure* 7*B–C* for representative images, *C* and *E* for quantification). A slight increase in proliferation was detected in AAV9-N1ICD transduced animals, which scored positive for BrdU and pH3(S10) (6.6% and 2.4%, respectively; *Figure* 7*A*, *Panels e–f* and *C* and *E* for quantification). Conversely, there was a net increase in BrdU+ animals in the AAV9-N1ICD(ΔC) and AAV9-N1ICD(ΔC)-HAT groups (∼14% in AAV9-N1ICD(ΔC) and 17.4% in AAV9-N1ICD(ΔC)-HAT, respectively to be compared to 3.3% of control animals), paralleled by a relevant increase of pH3(S10)+ cardiomyocytes (6.5% in AAV9-N1ICD(ΔC) and ∼9% in AAV9-N1ICD(ΔC)-HAT, respectively to be compared to ∼1% of control animals; *Figure* 7*A, Panels h-i, m-n* and *C* and *E* for quantification). High magnification representative images showing G2/M cells in resected hearts of mice transduced with AAV9-N1ICD(ΔC)-HAT are shown in Supplementary material online, *Figure S10, 7 (Panel A)* or 21 days (*Panel B*) after surgery.

Taken together these results support the conclusion that acetylation tunes Notch1 signalling *in vivo*: the net increase of NICD stability of the N1ICD(ΔC)-HAT protein widens the frame of cardiomyocyte proliferation, therefore enhancing tissue regeneration.

4. Discussion

Our results demonstrate that acetylation tightly controls the amplitude and duration of Notch signalling in neonatal rat cardiomyocytes. We report that a fraction of nuclear N1ICD is acetylated in neonatal rat cardiomyocytes upon stimulation by Jagged1 or in treatment with HDACs inhibitors. Acetylation impairs proteasomal-mediated degradation of the protein; as a consequence, its half-life is extended, and its transcriptional activity enhanced, resulting in sustained cardiomyocyte proliferation and protection from apoptosis. On the contrary, we show that Sirt1 acts as a negative modulator of Notch1 signalling; resveratrol treatment of cardiomyocytes completely reverts Notch1 acetylation, dampens its stability and significantly reduces its downstream signalling.

Notch stimulation obtained by NAM and (S)-35 and Notch inhibition observed after resveratrol treatment or Sirt1 overexpression consistently point out that class III HDACs act as suppressors of Notch activity in cardiomyocytes. In particular, Sirt1 inhibition increased acetylation, protein stability and transcriptional activity of Notch1 ensuing in the stimulation of cell proliferation. Conversely, treatment with resveratrol blocked acetylation, inhibited transcription and markedly suppressed cardiomyocyte proliferation. An obvious caveat of these studies is that both inhibition and activation of HDAC with drugs may have a pleiotropic effect on the cells, extending far beyond the regulation of Notch signalling. In this context, resveratrol, while being an inhibitor of Notch through Sirt1 activation, still exerted a strong protection from apoptosis of cultured cardiomyocytes. Different studies have shown that Sirt 1 acts as a key regulator of cell defences and survival in response to stress mainly acting through the FoxO transcription factors.[47,48] In particular, resveratrol was reported to inhibit hypoxia-induced apoptosis via the Sirt–FoxO1 pathway in H9c2 cardiomyocyte cells,[42] consistent with the capacity of Sirt1 to induce Mn-SOD expression under oxidative stress, observed in *Caenorhabditis elegans*,[49] and during chronic heart failure in rodents.[50] In our experiment, sustained expression of Sirt1 upon AAV6-mediated gene transfer in cardiomyocytes promoted N1ICD deaceylation and dramatically dampened its intracellular half-life, markedly suppressing cardiomyocyte proliferation. However, the effects of Sirt1 activation in the heart appear to have broader implications than regulating Notch1 stability and function, which are likely to be both context- and dose-dependent. In transgenic mouse hearts, mild to moderate expression of Sirt1 was shown to attenuate age-dependent increases in cardiac hypertrophy, whereas a high dose of Sirt1 increased oxidative stress and induced cardiomyopathy.[51] Furthermore, Sirt1 controls the amplitude and duration of Notch responses not only by negatively regulating Notch1 stability, but also by interfering with Notch-regulated gene transcription. In particular, Sirt1 takes part in the formation of a co-repressor complex, identified in flies and mammals, containing two chromatin-modifying enzymes, Sirt1 and LSD1, which jointly repress transcription of Hes1 through heterochromatin formation and

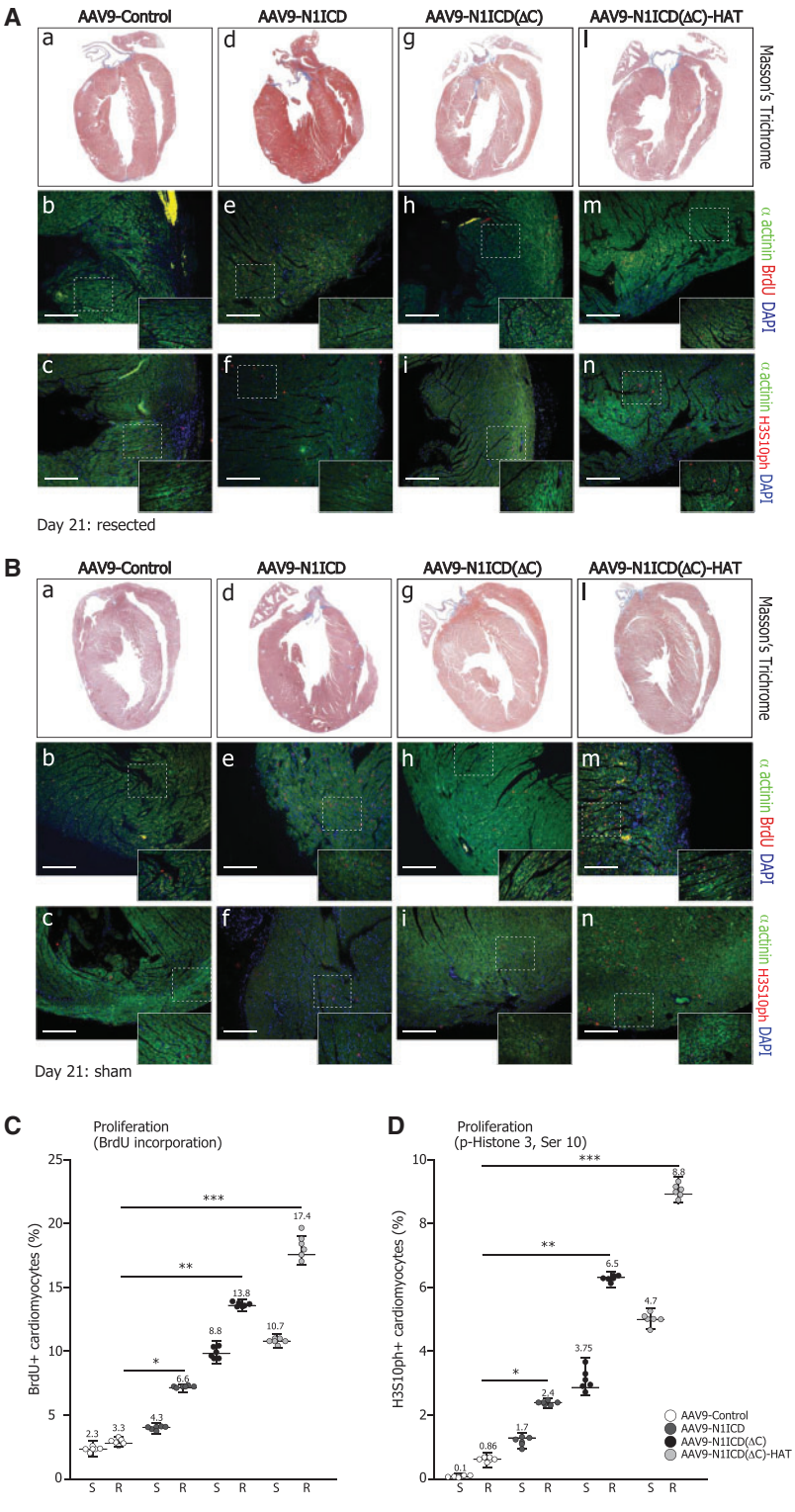

Figure 7 Acetylation of N1ICD enhances the regenerative potential of hearts 3 weeks after apical resection. (*A*) Representative images of resected hearts from mice transduced with AAV9-MCS (Control), AAV9-N1ICD, AAV9-N1ICD(ΔC), N1ICD(ΔC)-HAT 21 days after surgery. (*Panels a-d-g-l*) Histology of resected hearts 21 days after surgery and AAV transduction. Azan-Mallory trichrome staining of representative cross-sections of one heart/group ($n = 6$ per group). (*Panels b-e-h-m*) Representative images of BrdU+ cardiomyocytes in resected animals at day 21 after surgery and AAV-mediated gene transfer. (blue: Dapi; green: α-actinin; red: BrdU; scale bar: 100 μm), quantification in *C*. (*Panels c-f-i-n*) Representative images of pH3-Ser10+ cardiomyocytes in resected animals at Day 21 after surgery and AAV-mediated gene transfer (blue: Dapi; green: α actinin; red: phosho-H3Ser10; scale bar: 50 μM), quantification in *D*. (*B*) Same as in *Panel A* for Sham operated mice. (*C*) Quantification of of BrdU+ cardiomyocytes in sham and resected animals at Day 21 after surgery and AAV-mediated gene transfer. Data are mean ± SEM; $n = 6$ per group; two-way ANOVA, Bonferroni's multiple comparison test; $^{*}P < 0.05$, $^{**}P < 0.01$, $^{***}P < 0.001$ relative to AAV-MCS transduced animals, used as a control. S, Sham; R, Resected animals. (*D*) Same as in *Panel C* for phosho-H3Ser10+ cardiomyocytes.

chromatin compaction.[52] Thus, Sirt1 repression may enable the cellular Notch signalling pathway to sense and respond rapidly to local metabolic changes in energy and oxygen availability[53]; the regulation of Notch function in the heart most likely takes part in this broader scheme of regulation.

Similar considerations on the pleiotropic effect of drugs also apply to the evaluation of the effect of the class I and II HDAC inhibitor TSA on Notch function. While TSA treatment increased Notch acetylation and stability, it nonetheless inhibited cardiomyocyte proliferation. This cytostatic effect of TSA has also been reported in other cellular contexts. The drug is known to trigger G1 phase cell cycle arrest through inhibition of cyclin/CDK complexes and induction of p21 and p27, as well as by inactivation of the phosphatidylinositol-3-kinase/Akt, p38 MAPK and ERK1/2 pathways.[54,55] We, and others, have previously shown that these pathways are essential to drive the ex vivo proliferation of neonatal cardiomyocytes.[15,19,56]

A more specific insight into the role of acetylation in the regulation of Notch pathway activity in cardiomyocytes can be inferred by our AAV6-mediated gene transfer studies. By contrasting the effects of the full length, N1ICD protein with those of the C-terminal truncated mutant N1ICD(ΔC), we confirmed that the Notch1 PEST domain plays an essential role for the protein turnover also in cardiomyocytes. Of interest, the former protein showed an acetylation response superimposable with that of the endogenous receptor, while acetylation of N1ICD(ΔC) was insensitive to HDAC inhibitors and its half life was significantly longer. These results provide the first evidence that Notch1 turnover is tuned by acetylation in cardiac cells.

Interplay between protein stability and the levels of acetylation are well established for several cellular and viral proteins. Direct competition between acetylation and ubiquitination of the same lysine residues has been reported for p53,[57] Smad7,[58] SREBP1a,[59] and Runx3.[60] In the case of the c-Myc oncoprotein, p300-dependent acetylation regulates the protein turnover and its transcriptional activity.[61,62] Acetylation may also prevent protein ubiquitination and degradation due to the induction of conformational changes.[63] In the case of Notch1, work performed in endothelial cells has shown that acetylation indeed controls the protein level and thus Notch activity during angiogenesis in zebrafish and mice.[26] In contrast, in T-ALL cells, acetylation of Notch3 exerts opposite effects, since it induces its ubiquitination[38] similar to other proteins we have investigated in the past.[64,65] These observations reinforce the conclusion that protein acetylation is a modification that is broadly used in the cell to tune function and that its consequences are strictly protein- and context-dependent. Of note, post-translational protein modification by acetylation commonly occurs only on a fraction of a protein in the cells, which nevertheless is functionally active. Our own work in past years has shown that this is the case for the E2F1 transcription factor,[66] HIV-1 integrase,[67] CDK9,[45] CDC6,[68] and VEGFR2.[69] Thus, Notch1 adds to the list of proteins in which acetylation enhances activity, in this case by prolonging the protein's half life; even if a fraction of the protein is affected, this still has relevance in terms of biological effect.

A fusion protein between the Notch1 ICD, devoid of its PEST domain, and the catalytic domain of p300 [N1ICD(ΔC)-HAT] obtained by exploiting a genetic strategy we recently used to increase acetylation of HIV-1 integrase,[44] turned out to be constitutively acetylated in cardiomyocytes. This protein was far more stable and thus acted as a strong Notch pathway activator. In particular, N1ICD(ΔC)-HAT was very powerful in both protecting neonatal cardiomyocytes from apoptosis, induced by either doxorubicin or low oxygen tension, and in driving their proliferation. Notch signalling was reported to promote cell survival in various cellular settings, including cancer cells[70] and T-cell lines.[71] This protective role of the pathway is also established in the heart: in our previous work we showed that the Notch pathway inhibitor DAPT increased cardiomyocyte apoptosis, while AAV-driven overexpression of N1-ICD exerted a protective effect.[15] Consistently, the heart-specific Notch1 deletion triggered increased fibrosis and decreased cardiac function by accelerating cardiomyocyte loss,[16] while Notch signalling protected cardiomyocytes after ischemic injury.[19,72]

The capacity of N1ICD(ΔC)-HAT to drive massive neonatal cardiomyocyte proliferation is even more intriguing than its strong anti-apoptotic effect. In mammals, cardiomyocyte proliferation rapidly ceases after birth and a highly regulated sequence of events trigger differentiation and hypertrophic growth of these cells in the postnatal life.[73] While the molecular mechanisms underlying this transition are the current focus of several laboratories, the remarkable proliferative effect observed after N1ICD(ΔC)-HAT gene transfer strongly support the conclusion that neonatal cardiomyocyte proliferation is under the positive control of the Notch pathway.[15–18] Cells expressing this protein were able to undergo division up to 2 weeks after plating, with transduction triggering the formation of clusters of cardiomyocytes positive for Edu, for histone H3 serine 10 phosphorylation (a marker of mitosis) and for localization of Aurora B kinase in midbodies even after 2 weeks of culture.

Besides highlighting the importance of acetylation as a rheostat for the regulation of Notch signalling, the N1ICD(ΔC)-HAT fusion protein represents an interesting transgene to drive cardiac cell proliferation *in vivo*. Experimental evidence in zebrafish shows that regeneration of the ventricle upon resection requires active Notch signalling,[22,74] consistent with the requirement of the Notch pathway for cardiac repair throughout the fish life.[23] In higher vertebrates, there is a conserved propensity for Notch-expressing cells to become active following injury.[19,20] This activation occurs both in the mouse epicardium, where Notch-expressing cells are amplified and increasingly adopt a fibroblast cell fate after damage,[75] as well as in cardiomyocytes, in which Notch signalling components exert a cardioprotective after stress.[16,76] As far as proliferation is concerned, however, previous work from our laboratory has shown that Notch pathway activation indeed regulates cardiomyocyte proliferation during the early postnatal life,[15] but is largely ineffective in driving cardiac regeneration in adults, due to permanent, suppressive epigenetic modification at Notch responsive promoters.[24] For this reason, here we tested the regenerative potency of the N1ICD(ΔC)-HAT fusion protein in a model of apical resection in neonatal mice hearts.[77]

The results obtained using the constitutively acetylated N1ICD(ΔC)-HAT in neonatal hearts were remarkable in terms of amplification of the cardiomyocyte proliferation and cardiac regeneration responses. In the proliferation-compliant background of the neonatal mouse heart, the sustained activation of the Notch pathway triggered a massive increase in the number of BrdU+, pH3(S10)+ cardiomyocytes, even in sham animals, by all three Notch vectors and, in particular, by N1ICD(ΔC)-HAT. This last vector was capable to stimulate cardiomyocyte proliferation up to 3 weeks after apical resection, a notable result considering that the regenerative-responsive window for cardiac regeneration normally lasts less than 7 days in the mouse.[77] Of note, the extent of cardiomyocytes incorporating BrdU after apical resection, in the absence of vector injection, was relatively more modest in our experiments compared to that reported by Porrello *et al.*[30] This is most likely because we started BrdU administration 5 days after resection, compared to 1 day in Porrello *et al.*,[30] thus probably missing the early replicative events after damage. The marked pro-proliferative effect of our Notch vectors, therefore, is even more striking considering our experimental settings.

Finally, it appears worth mentioning that the significant increase in mitotic cells, as judged by phospho-histone H3 labelling, observed after Notch overexpression, was not paralleled by augmented heart size. This might either indicate that a few of the mitotic events lead to multinucleation consequent to failed cytokinesis or that the Notch vectors-induced cell hyperplasia parallels a decrease in physiological hypertrophy during of cardiac growth. This would constitute an interesting matter for future investigations.

Collectively, our studies demonstrate that the cardiomyocyte proliferative renewal is exquisitely sensitive to stimulation by Notch signalling and that Notch post-translational modification by acetylation is a powerful amplifier of this effect both *in vitro* and *in vivo*.

Acknowledgements

The authors are grateful to M. Potente, F. Ishikawa, I. Prudovsky, R. Kopan, S.D. Hayward, R. Kageyama, A. Cereseto, and G. Weinmaster for kindly providing plasmids and constructs; to Marina Dapas and Michela Zotti for their outstanding technical support and to Suzanne Kerbavcic for excellent editorial assistance.

Conflict of interest: none declared.

Funding

This work was supported by the European Research Council (ERC) [Advanced Grant 250124]; the Leducq Foundation Transatlantic Network of Excellence [grant 14CVD04]; the Fondazione CRTrieste [Project CTC], Trieste, Italy and the Italian Ministry of Health [RF-2011-02348164 "Cardiorigen"].

References

1. Burton PB, Raff MC, Kerr P, Yacoub MH, Barton PJ. An intrinsic timer that controls cell-cycle withdrawal in cultured cardiac myocytes. *Dev Biol* 1999;**216**:659–670.
2. Winick M, Noble A. Quantitative changes in DNA, RNA, and protein during prenatal and postnatal growth in the rat. *Dev Biol* 1965;**12**:451–466.
3. Li F, Wang X, Capasso JM, Gerdes AM. Rapid transition of cardiac myocytes from hyperplasia to hypertrophy during postnatal development. *J Mol Cell Cardiol* 1996;**28**: 1737–1746.
4. Bergmann O, Bhardwaj RD, Bernard S, Zdunek S, Barnabé-Heider F, Walsh S, Zupicich J, Alkass K, Buchholz BA, Druid H, Jovinge S, Frisén J. Evidence for cardiomyocyte renewal in humans. *Science* 2009;**324**:98–102.
5. Kajstura J, Urbanek K, Perl S, Hosoda T, Zheng H, Ogorek B, Ferreira-Martins J, Goichberg P, Rondon-Clavo C, Sanada F, D'Amario D, Rota M, Del Monte F, Orlic D, Tisdale J, Leri A, Anversa P. Cardiomyogenesis in the adult human heart. *Circ Res* 2010;**107**:305–315.
6. Senyo SE, Steinhauser ML, Pizzimenti CL, Yang VK, Cai L, Wang M, Wu TD, Guerquin-Kern JL, Lechene CP, Lee RT. Mammalian heart renewal by pre-existing cardiomyocytes. *Nature* 2013;**493**:433–436.
7. Birks EJ. Molecular changes after left ventricular assist device support for heart failure. *Circ Res* 2013;**113**:777–791.
8. Roger VL. Epidemiology of heart failure. *Circ Res* 2013;**113**:646–659.
9. Bray SJ. Notch signalling: a simple pathway becomes complex. *Nat Rev Mol Cell Biol* 2006;**7**:678–689.
10. Borggrefe T, Oswald F. The Notch signaling pathway: transcriptional regulation at Notch target genes. *Cell Mol Life Sci* 2009;**66**:1631–1646.
11. Kopan R, Ilagan MX. The canonical Notch signaling pathway: unfolding the activation mechanism. *Cell* 2009;**137**:216–233.
12. de la Pompa JL, Epstein JA. Coordinating tissue interactions: Notch signaling in cardiac development and disease. *Dev Cell* 2012;**22**:244–254.
13. Niessen K, Karsan A. Notch signaling in cardiac development. *Circ Res* 2008;**102**: 1169–1181.
14. Pedrazzini T. Control of cardiogenesis by the notch pathway. *Trends Cardiovasc Med* 2007;**17**:83–90.
15. Collesi C, Zentilin L, Sinagra G, Giacca M. Notch1 signaling stimulates proliferation of immature cardiomyocytes. *J Cell Biol* 2008;**183**:117–128.
16. Croquelois A, Domenighetti AA, Nemir M, Lepore M, Rosenblatt-Velin N, Radtke F, Pedrazzini T. Control of the adaptive response of the heart to stress via the Notch1 receptor pathway. *J Exp Med* 2008;**205**:3173–3185.
17. Campa VM, Gutierrez-Lanza R, Cerignoli F, Diaz-Trelles R, Nelson B, Tsuji T, Barcova M, Jiang W, Mercola M. Notch activates cell cycle reentry and progression in quiescent cardiomyocytes. *J Cell Biol* 2008;**183**:129–141.
18. Urbanek K, Cabral-da-Silva MC, Ide-Iwata N, Maestroni S, Delucchi F, Zheng H, Ferreira-Martins J, Ogorek B, D'Amario D, Bauer M, Zerbini G, Rota M, Hosoda T, Liao R, Anversa P, Kajstura J, Leri A. Inhibition of notch1-dependent cardiomyogenesis leads to a dilated myopathy in the neonatal heart. *Circ Res* 2010;**107**:429–441.
19. Gude NA, Emmanuel G, Wu W, Cottage CT, Fischer K, Quijada P, Muraski JA, Alvarez R, Rubio M, Schaefer E, Sussman MA. Activation of Notch-mediated protective signaling in the myocardium. *Circ Res* 2008;**102**:1025–1035.
20. Kratsios P, Catela C, Salimova E, Huth M, Berno V, Rosenthal N, Mourkioti F. Distinct roles for cell-autonomous Notch signaling in cardiomyocytes of the embryonic and adult heart. *Circ Res* 2010;**106**:559–572.
21. Øie E, Sandberg WJ, Ahmed MS, Yndestad A, Lærum OD, Attramadal H, Aukrust P, Eiken HG. Activation of Notch signaling in cardiomyocytes during post-infarction remodeling. *Scand Cardiovasc J* 2010;**44**:359–366.
22. Raya A, Koth CM, Buscher D, Kawakami Y, Itoh T, Raya RM, Sternik G, Tsai HJ, Rodriguez-Esteban C, Izpisua-Belmonte JC. Activation of Notch signaling pathway precedes heart regeneration in zebrafish. *Proc Natl Acad Sci USA* 2003;**100**: 11889–11895.
23. Zhang R, Han P, Yang H, Ouyang K, Lee D, Lin YF, Ocorr K, Kang G, Chen J, Stainier DY, Yelon D, Chi NC. In vivo cardiac reprogramming contributes to zebrafish heart regeneration. *Nature* 2013;**498**:497–501.
24. Felician G, Collesi C, Lusic M, Martinelli V, Ferro MD, Zentilin L, Zacchigna S, Giacca M. Epigenetic modification at Notch responsive promoters blunts efficacy of inducing Notch pathway reactivation after myocardial infarction. *Circ Res* 2014;**115**:636–649.
25. Tien AC, Rajan A, Bellen HJ. A Notch updated. *J Cell Biol* 2009;**184**:621–629.
26. Guarani V, Deflorian G, Franco CA, Kruger M, Phng LK, Bentley K, Toussaint L, Dequiedt F, Mostoslavsky R, Schmidt MH, Zimmermann B, Brandes RP, Mione M, Westphal CH, Braun T, Zeiher AM, Gerhardt H, Dimmeler S, Potente M. Acetylation-dependent regulation of endothelial Notch signalling by the SIRT1 deacetylase. *Nature* 2011;**473**:234–238.
27. Brooks CL, Gu W. How does SIRT1 affect metabolism, senescence and cancer? *Nat Rev Cancer* 2009;**9**:123–128.
28. Finkel T, Deng CX, Mostoslavsky R. Recent progress in the biology and physiology of sirtuins. *Nature* 2009;**460**:587–591.
29. Feige JN, Auwerx J. Transcriptional targets of sirtuins in the coordination of mammalian physiology. *Curr Opin Cell Biol* 2008;**20**:303–309.
30. Porrello ER, Mahmoud AI, Simpson E, Hill JA, Richardson JA, Olson EN, Sadek HA. Transient regenerative potential of the neonatal mouse heart. *Science* 2011;**331**: 1078–1080.
31. Bish RA, Fregoso OI, Piccini A, Myers MP. Conjugation of complex polyubiquitin chains to WRNIP1. *J Proteome Res* 2008;**7**:3481–3489.
32. Arsic N, Zacchigna S, Zentilin L, Ramirez-Correa G, Pattarini L, Salvi A, Sinagra G, Giacca M. Vascular endothelial growth factor stimulates skeletal muscle regeneration in vivo. *Mol Ther* 2004;**10**:844–854.
33. Gao GP, Alvira MR, Wang L, Calcedo R, Johnston J, Wilson JM. Novel adeno-associated viruses from rhesus monkeys as vectors for human gene therapy. *Proc Natl Acad Sci USA* 2002;**99**:11854–11859.
34. Zentilin L, Marcello A, Giacca M. Involvement of cellular double-strand DNA break-binding proteins in processing of recombinant adeno-associated virus (AAV) genome. *J Virol* 2001;**75**:12279–12287.
35. Howitz KT, Bitterman KJ, Cohen HY, Lamming DW, Lavu S, Wood JG, Zipkin RE, Chung P, Kisielewski A, Zhang LL, Scherer B, Sinclair DA. Small molecule activators of sirtuins extend Saccharomyces cerevisiae lifespan. *Nature* 2003;**425**:191–196.
36. Wood JG, Rogina B, Lavu S, Howitz K, Helfand SL, Tatar M, Sinclair D. Sirtuin activators mimic caloric restriction and delay ageing in metazoans. *Nature* 2004;**430**:686–689.
37. Solomon JM, Pasupuleti R, Xu L, McDonagh T, Curtis R, DiStefano PS, Huber LJ. Inhibition of SIRT1 catalytic activity increases p53 acetylation but does not alter cell survival following DNA damage. *Mol Cell Biol* 2006;**26**:28–38.
38. Palermo R, Checquolo S, Giovenco A, Grazioli P, Kumar V, Campese AF, Giorgi A, Napolitano M, Canettieri G, Ferrara G, Schinina ME, Maroder M, Frati L, Gulino A, Vacca A, Screpanti I. Acetylation controls Notch3 stability and function in T-cell leukemia. *Oncogene* 2012;**31**:3807–3817.
39. Popko-Scibor AE, Lindberg MJ, Hansson ML, Holmlund T, Wallberg AE. Ubiquitination of Notch1 is regulated by MAML1-mediated p300 acetylation of Notch1. *Biochem Biophys Res Commun* 2011;**416**:300–306.
40. Jarriault S, Brou C, Logeat F, Schroeter EH, Kopan R, Israel A. Signalling downstream of activated mammalian Notch. *Nature* 1995;**377**:355–358.
41. Hsieh JJ, Henkel T, Salmon P, Robey E, Peterson MG, Hayward SD. Truncated mammalian Notch1 activates CBF1/RBPJk-repressed genes by a mechanism resembling that of Epstein-Barr virus EBNA2. *Mol Cell Biol* 1996;**16**:952–959.

42. Chen CJ, Yu W, Fu YC, Wang X, Li JL, Wang W. Resveratrol protects cardiomyocytes from hypoxia-induced apoptosis through the SIRT1-FoxO1 pathway. *Biochem Biophys Res Commun* 2009;**378**:389–393.
43. Lovric J, Mano M, Zentilin L, Eulalio A, Zacchigna S, Giacca M. Terminal differentiation of cardiac and skeletal myocytes induces permissivity to AAV transduction by relieving inhibition imposed by DNA damage response proteins. *Mol Ther* 2012;**20**: 2087–2097.
44. Allouch A, Di Primio C, Alpi E, Lusic M, Arosio D, Giacca M, Cereseto A. The TRIM family protein KAP1 inhibits HIV-1 integration. *Cell Host Microbe* 2011;**9**: 484–495.
45. Sabo A, Lusic M, Cereseto A, Giacca M. Acetylation of conserved lysines in the catalytic core of cyclin-dependent kinase 9 inhibits kinase activity and regulates transcription. *Mol Cell Biol* 2008;**28**:2201–2212.
46. Boni A, Urbanek K, Nascimbene A, Hosoda T, Zheng H, Delucchi F, Amano K, Gonzalez A, Vitale S, Ojaimi C, Rizzi R, Bolli R, Yutzey KE, Rota M, Kajstura J, Anversa P, Leri A. Notch1 regulates the fate of cardiac progenitor cells. *Proc Natl Acad Sci USA* 2008;**105**:15529–15534.
47. Motta MC, Divecha N, Lemieux M, Kamel C, Chen D, Gu W, Bultsma Y, McBurney M, Guarente L. Mammalian SIRT1 represses forkhead transcription factors. *Cell* 2004; **116**:551–563.
48. Brunet A, Sweeney LB, Sturgill JF, Chua KF, Greer PL, Lin Y, Tran H, Ross SE, Mostoslavsky R, Cohen HY, Hu LS, Cheng HL, Jedrychowski MP, Gygi SP, Sinclair DA, Alt FW, Greenberg ME. Stress-dependent regulation of FOXO transcription factors by the SIRT1 deacetylase. *Science* 2004;**303**:2011–2015.
49. Kops GJ, Dansen TB, Polderman PE, Saarloos I, Wirtz KW, Coffer PJ, Huang TT, Bos JL, Medema RH, Burgering BM. Forkhead transcription factor FOXO3a protects quiescent cells from oxidative stress. *Nature* 2002;**419**:316–321.
50. Tanno M, Kuno A, Yano T, Miura T, Hisahara S, Ishikawa S, Shimamoto K, Horio Y. Induction of manganese superoxide dismutase by nuclear translocation and activation of SIRT1 promotes cell survival in chronic heart failure. *J Biol Chem* 2010;**285**: 8375–8382.
51. Alcendor RR, Gao S, Zhai P, Zablocki D, Holle E, Yu X, Tian B, Wagner T, Vatner SF, Sadoshima J. Sirt1 regulates aging and resistance to oxidative stress in the heart. *Circ Res* 2007;**100**:1512–1521.
52. Mulligan P, Yang F, Di Stefano L, Ji J-Y, Ouyang J, Nishikawa JL, Toiber D, Kulkarni M, Wang Q, Najafi-Shoushtari SH, Mostoslavsky R, Gygi SP, Gill G, Dyson NJ, Näär AM. A SIRT1-LSD1 corepressor complex regulates Notch target gene expression and development. *Mol Cell* 2011;**42**:689–699.
53. Vaquero A, Reinberg D. Calorie restriction and the exercise of chromatin. *Genes Dev* 2009;**23**:1849–1869.
54. Majumdar G, Rooney RJ, Johnson IM, Raghow R. Panhistone deacetylase inhibitors inhibit proinflammatory signaling pathways to ameliorate interleukin-18-induced cardiac hypertrophy. *Physiol Genomics* 2011;**43**:1319–1333.
55. Chen X, Xiao W, Chen W, Luo L, Ye S, Liu Y. The epigenetic modifier trichostatin A, a histone deacetylase inhibitor, suppresses proliferation and epithelial-mesenchymal transition of lens epithelial cells. *Cell Death Dis* 2013;**4**:e884.
56. Beigi F, Schmeckpeper J, Pow-Anpongkul P, Payne JA, Zhang L, Zhang Z, Huang J, Mirotsou M, Dzau VJ. C3orf58, a novel paracrine protein, stimulates cardiomyocyte cell-cycle progression through the PI3K-AKT-CDK7 pathway. *Circ Res* 2013;**113**: 372–380.
57. van Leeuwen IMM, Higgins M, Campbell J, McCarthy AR, Sachweh MCC, Navarro AM, Laín S. Modulation of p53 C-terminal acetylation by mdm2, p14ARF, and cytoplasmic SirT2. *Mol Cancer Ther* 2013;**12**:471–480.
58. Gronroos E, Hellman U, Heldin CH, Ericsson J. Control of Smad7 stability by competition between acetylation and ubiquitination. *Mol Cell* 2002;**10**:483–493.
59. Giandomenico V, Simonsson M, Gronroos E, Ericsson J. Coactivator-dependent acetylation stabilizes members of the SREBP family of transcription factors. *Mol Cell Biol* 2003;**23**:2587–2599.
60. Jin YH, Jeon EJ, Li QL, Lee YH, Choi JK, Kim WJ, Lee KY, Bae SC. Transforming growth factor-beta stimulates p300-dependent RUNX3 acetylation, which inhibits ubiquitination-mediated degradation. *J Biol Chem* 2004;**279**:29409–29417.
61. Patel JH, Du Y, Ard PG, Phillips C, Carella B, Chen CJ, Rakowski C, Chatterjee C, Lieberman PM, Lane WS, Blobel GA, McMahon SB. The c-MYC oncoprotein is a substrate of the acetyltransferases hGCN5/PCAF and TIP60. *Mol Cell Biol* 2004;**24**: 10826–10834.
62. Faiola F, Liu X, Lo S, Pan S, Zhang K, Lymar E, Farina A, Martinez E. Dual regulation of c-Myc by p300 via acetylation-dependent control of Myc protein turnover and coactivation of Myc-induced transcription. *Mol Cell Biol* 2005;**25**:10220–10234.
63. Caron C, Boyault C, Khochbin S. Regulatory cross-talk between lysine acetylation and ubiquitination: role in the control of protein stability. *Bioessays* 2005;**27**:408–415.
64. Galbiati L, Mendoza-Maldonado R, Gutierrez MI, Giacca M. Regulation of E2F-1 after DNA damage by p300-mediated acetylation and ubiquitination. *Cell Cycle* 2005;**4**:930–939.
65. Mateo F, Vidal-Laliena M, Canela N, Zecchin A, Martinez-Balbas M, Agell N, Giacca M, Pujol MJ, Bachs O. The transcriptional co-activator PCAF regulates cdk2 activity. *Nucleic Acids Res* 2009;**37**:7072–7084.
66. Marzio G, Wagener C, Gutierrez MI, Cartwright P, Helin K, Giacca M. E2F family members are differentially regulated by reversible acetylation. *J Biol Chem* 2000;**275**: 10887–10892.
67. Cereseto A, Manganaro L, Gutierrez MI, Terreni M, Fittipaldi A, Lusic M, Marcello A, Giacca M. Acetylation of HIV-1 integrase by p300 regulates viral integration. *EMBO J* 2005;**24**:3070–3081.
68. Paolinelli R, Mendoza-Maldonado R, Cereseto A, Giacca M. Acetylation by GCN5 regulates CDC6 phosphorylation in the S phase of the cell cycle. *Nat Struct Mol Biol* 2009;**16**:412–420.
69. Zecchin A, Pattarini L, Gutierrez MI, Mano M, Mai A, Valente S, Myers MP, Pantano S, Giacca M. Reversible acetylation regulates vascular endothelial growth factor receptor-2 activity. *J Mol Cell Biol* 2014;**6**:116–127.
70. Mungamuri SK, Yang X, Thor AD, Somasundaram K. Survival signaling by Notch1: mammalian target of rapamycin (mTOR)-dependent inhibition of p53. *Cancer Res* 2006;**66**:4715–4724.
71. Jehn BM, Bielke W, Pear WS, Osborne BA. Cutting edge: protective effects of notch-1 on TCR-induced apoptosis. *J Immunol* 1999;**162**:635–638.
72. Zhou XL, Wan L, Xu QR, Zhao Y, Liu JC. Notch signaling activation contributes to cardioprotection provided by ischemic preconditioning and postconditioning. *J Transl Med* 2013;**11**:251.
73. van Amerongen M, Engel F. Induction of cardiomyocyte proliferation. In FB Engels (ed). *Heart Regeneration Stem Cells and Beyond*. World Scientific Collection, 2012. pp. 105–134.
74. Zhao L, Borikova AL, Ben-Yair R, Guner-Ataman B, MacRae CA, Lee RT, Burns CG, Burns CE. Notch signaling regulates cardiomyocyte proliferation during zebrafish heart regeneration. *Proc Natl Acad Sci USA* 2014;**111**:1403–1408.
75. Russell JL, Goetsch SC, Gaiano NR, Hill JA, Olson EN, Schneider JW. A dynamic notch injury response activates epicardium and contributes to fibrosis repair. *Circ Res* 2011;**108**:51–59.
76. Nemir M, Metrich M, Plaisance I, Lepore M, Cruchet S, Berthonneche C, Sarre A, Radtke F, Pedrazzini T. The Notch pathway controls fibrotic and regenerative repair in the adult heart. *Eur Heart J* 2014;**35**:2174–2185.
77. Porrello ER, Johnson BA, Aurora AB, Simpson E, Nam YJ, Matkovich SJ, Dorn GW 2nd, van Rooij E, Olson EN. MiR-15 family regulates postnatal mitotic arrest of cardiomyocytes. *Circ Res* 2011;**109**:670–679.